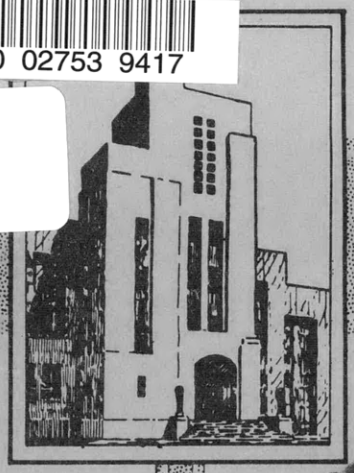

NAVY DEPARTMENT

DAVID TAYLOR MODEL BASIN

HYDROMECHANICS

○

AERODYNAMICS

○

STRUCTURAL MECHANICS

○

APPLIED MATHEMATICS

THE DESIGN AND PERFORMANCE OF SUPERCAVITATING PROPELLERS

by

A.J. Tachmindji, W.B. Morgan,
M.L. Miller, and R. Hecker

HYDROMECHANICS LABORATORY

RESEARCH AND DEVELOPMENT REPORT

February 1957 Report C-807

SUMMARY

STATEMENT OF PROBLEM

This investigation was established to determine the feasibility of adopting supercavitating sections to propellers for high-speed craft and to develop a design method for such propellers.

This report also covers a number of experimental results.

CONCLUSIONS

1. The results show that supercavitating propellers are feasible and that the performance is considerably improved over that of heavily-cavitating conventional propellers.

2. The design method developed in this report gave satisfactory results for the propellers investigated.

3. Comparison of the full-scale performance and model performance of one supercavitating propeller design showed that the scale effect, if any, was within the experimental accuracy of the results.

THE DESIGN AND PERFORMANCE OF SUPERCAVITATING PROPELLERS

by

A.J. Tachmindji, W.B. Morgan,
M.L. Miller, and R. Hecker

February 1957 Report C-807

TABLE OF CONTENTS

LIST OF ILLUSTRATIONS

NOTATION

A_1	$\frac{8}{5\pi} C_{L_0}$
B	Coefficient for determining pressure face ordinates
C_D	Total drag coefficient
$(C_D)_f$	Frictional drag coefficient
$(C_D)_p$	Potential drag coefficient
C_L	Design lift coefficient
C_{L_0}	Lift coefficient from camber
D	Propeller diameter
E	Coefficient for determining pressure face ordinates
e	Propeller efficiency $\left(\frac{T V_a}{2\pi Qn}\right)$
F and F'	Coefficients for determining section thickness
g	Acceleration of gravity
H	Absolute pressure at shaft centerline minus vapor pressure in feet of water $(h + h_a - h_v)$
h	Distance shaft centerline is below water surface
h_a	Atmospheric pressure (33 ft of sea water)
h_v	Vapor pressure of water (0.5 ft of sea water at 59 deg F)
J	Speed coefficient $\left(\frac{V_a}{nD}\right)$
K	Correction factor for finite cavitation number
K_q	Torque coefficient $\left(\frac{Q}{\rho n^2 D^5}\right)$
K_t	Thrust coefficient $\left(\frac{T}{\rho n^2 D^4}\right)$
l	Section chord length
N and N'	Coefficients for determining section thickness
n	Revolutions per unit time
P/D	Pitch ratio
Q	Propeller torque
R	Maximum propeller radius

R_e	Reynolds number $\left(l_{0.7}\ \frac{\sqrt{V_a^2 + (0.7\pi n D)^2}}{\nu}\right)$
r	Radius of any propeller blade section
shp	Shaft horsepower $\left(\frac{2\pi Q n}{550}\right)$
T	Propeller thrust
t	Cavity thickness
thp	Thrust horsepower $\left(\frac{T\ V_a}{550}\right)$
u_t	Tangential component of induced velocity
V_a	Speed of advance
V_k	Speed of advance in knots
V_r	Inflow velocity to section $\left(\frac{x\pi n D - \frac{u_t}{2}}{\cos\beta_i}\right)$
x	Nondimensional radius $\left(\frac{r}{R}\right)$
x_l	Fractional distance along chord measured from leading edge
y	Face ordinate measured perpendicular to nose-tail line
α	Design angle of attack
α_0	Angle of attack for zero lift
α_1	Angle of attack from friction and ideal angle of attack
α_2	Angle of attack from lifting surface effect
α_i	Ideal angle of attack
β_i	Hydrodynamic pitch angle
ϵ	Drag-lift ratio
θ	Geometric angle of attack
ρ	Density of fluid
σ	Cavitation number based on propeller speed of advance $\left(\frac{2gH}{V_a^2}\right)$
σ_x	Cavitation number based on inflow velocity to section $\left(\frac{2gH}{V_r^2}\right)$
ν	Kinematic viscosity

ABSTRACT

A design method for supercavitating propellers is outlined and results of a number of tests are presented. Evaluation of the results shows that supercavitating propellers are feasible as a propulsion device for high-speed craft.

INTRODUCTION

The increasing speeds of naval vessels and underwater missiles have introduced a number of problems in the design of propellers and are imposing stringent limitations upon the configuration of the propulsion mechanism. Of these difficulties the most important one is propeller cavitation and its associated effects on performance, noise, and erosion. A number of investigations have been performed on other types of propulsion mechanisms, such as pump-jets and shrouded propellers, aimed towards delaying the inception speed of cavitation. It is, however, apparent that for vehicles operating at very high speeds (50 knots and above) suppression of cavitation becomes impossible even if the propulsion mechanism is lightly loaded.

An investigation was therefore initiated at the David Taylor Model Basin as part of the Fundamental Research Program to determine the feasibility of designing and developing a propeller which could be used for very high speed craft and would operate with fully developed cavitation. Such a propeller has the backs of its blades completely enclosed within a vapor cavity which originates at the leading edge of the blade. This type of propeller is usually known as a supercavitating (SC) propeller.

The effects of high-speed operation can be divided into three areas:

1. Effect on performance. A conventional propeller operated with fully developed cavitation will, in general experience a decrease in the thrust and torque coefficients accompanied by a reduction in efficiency. This problem has led to a considerable interest in the application of an efficient fully cavitating section to propeller design.

2. Acoustic characteristics. It is well known that the noise characteristics of conventional propellers are greatly affected by the presence of tip vortices or blade surface cavitation. It is, therefore, important to determine the noise characteristics of a SC propeller when the cavity collapses beyond the trailing edge of the blade. It is of interest to determine also whether air would diffuse into the vapor cavity in such a way as to materially improve the noise characteristics.

3. Metallurgical effects (erosion). The collapse of the vapor bubble beyond the trailing edge may result in a reduction of the cavitation erosion encountered with conventional blades.

The purpose of the initial program was to evaluate the effects of supercavitation on performance and to determine the feasibility of this type of propulsion. This report outlines the design method which has been used for these evaluations and presents the results of a number of tests.

PURPOSE OF INITIAL PROGRAM

Following the development of low-drag supercavitating (SC) sections for zero cavitation index which was performed by Tulin[1], it was decided to use these sections in determining the feasibility of SC propellers. It was also necessary to develop a design procedure, determine the cavitation index at which such propellers can be operated, and develop theoretical methods for determining the operating characteristics. Furthermore, it was necessary to check that no scale effects are present for fully cavitating flows and that the similitude laws between model and full scale would be satisfactory.

For the purpose of developing a design method and checking the performance characteristics, it was decided that a high speed, high rpm propeller would be designed and tested in the 24-Inch Variable Pressure Water Tunnel at the David Taylor Model Basin. Based on the results of these tests a second propeller was designed for full-scale application. A model of the same design was also manufactured and tested to determine any possible scale effects. The second design was based on the operating characteristics of the R-100 Canadian hydrofoil boat and tested on that vessel.

SUPERCAVITATING SECTIONS

Before outlining the design method used in the development of SC propellers, it is desirable to review the available data on these sections with a view to using such data for propeller operation. The work done by Tulin[1] in determining an optimum section is limited to zero cavitation index and the section is not necessarily an absolute optimum, but only the optimum section within a series of similar shapes. Tulin extended his results for the case of finite cavitation number[2] and determined the magnitude of this effect on the characteristics of flat faced sections.

Further work along the same lines has also been conducted by Wu[3], who developed the exact theory for finite cavitation number by considering an analysis based on the Roshko model. The effect of finite and zero cavitation index has also been investigated by Hug[4]. The results obtained by all three investigations are essentially similar within the limits of their assumptions. In the application of these sections to propeller development, however, Tulin's work was primarily followed since this was the only available information at the time the designs were contemplated.

Tulin's work gives essentially the ordinates of the camber line and the cavity shape for $\sigma = 0$. It is found, however, that for angles of attack of the order of the ideal angle of attack (α_i), the cavity ordinates become negative, which means that physically the cavity cannot exist on the back of the section. There is, therefore, a minimum angle of attack at which these sections can operate.

---

[1]References are listed on page 31.

In order to determine any differences which may exist in the theoretical results, two-dimensional tests were run on a specific section[5]. On the basis of these experimental data a correction factor has been determined for sections operating at finite cavitation numbers in a real fluid.

DESIGN CONSIDERATIONS

The design of SC propellers has been accomplished by using the theoretically derived sections in the propeller design method presently used at DTMB[6]. Based on this design method, an evaluation of the performance characteristics for these propellers was possible. This resulted in certain recommendations as to the range of application and conditions for which their performance characteristics are superior to those of conventional propellers.

In order to insure that the cavity on the back of the blade is fully developed it is necessary to keep the cavitation number of the section as low as possible. Water-tunnel tests on SC propellers have indicated that if σ_x at $0.7R$ is less than 0.045 this condition can be achieved. In order to reach this low cavitation index the propeller has to be operated at a high speed of advance and/or high rpm. At moderate forward speeds, 35 to 50 knots, and reasonable diameters this means that the propeller must be operated at high rotational speeds. Since this may result in a low pitch and the performance of the propeller is dependent on pitch ratio, or design speed coefficient J, an inherently low efficiency may have to be accepted. It is, therefore, desirable that the design speed be as high as possible in order to achieve a considerable gain in efficiency over conventional propellers. Figure 1 gives a plot of H/V_k^2 (which is proportional to the propeller cavitation index) against speed coefficient and indicates the range of practicability for SC propellers. Region I shows the area in which the design of SC propellers is practical, Region II is the area in which they are marginal, Region III is the area in which most conventional propellers operate, and Region IV is the area undesirable for any design because of the resulting low efficiency. It should be noted that for the same H/V_k^2 a propeller of conventional design working in Region III would normally be more efficient than a SC propeller operating in Region I.

The design of a SC propeller is, to a certain extent, limited by the maximum stress which can be accepted at the blade surface. Although the computed stress is only a nominal value, it is desirable to maintain the stress as low as possible. The final design is, therefore, dictated by both hydrodynamic and stress considerations. For a given cavitation index and section lift coefficient it is possible to determine the shape of the camber line and the thickness of the cavity. The section to be used is then fitted between these two limits. In order to insure that face cavitation does not develop where irregularities occur in the flow, it is also necessary to develop part of the lift by using some angle of attack. From available experimental results[7,8] it can be concluded that the lift coefficient C_L should be equal to or less than 10 percent of the design angle of attack α.

$$C_L \leqq 0.1\,\alpha \qquad [1]$$

where α is the design angle of attack in degrees.

The design of an optimum SC propeller for a given set of operating conditions leads to a rather complex investigation resulting from a compromise between the best hydrodynamic features and the most acceptable stress limits. In the following paragraph the effects of individual parameters will be briefly described. Given the conditions of thrust, speed, and rpm, it is necessary to determine the optimum propeller for a given nominal stress limit. By assuming the diameter and number of blades, it is possible to determine the radial distribution of $C_L l/D$ where C_L is the section lift coefficient, l is the chord of the section, and D is the propeller diameter. It is now necessary to assume a blade outline which will allow the determination of C_L. The hydrodynamic performance and structural characteristics of the propeller can then be computed. The following considerations should be borne in mind:

1. For minimum friction drag, the chord l should be as small as possible.

2. For minimum potential drag, the chord l should be as large as possible, thus resulting in a small value of C_L.

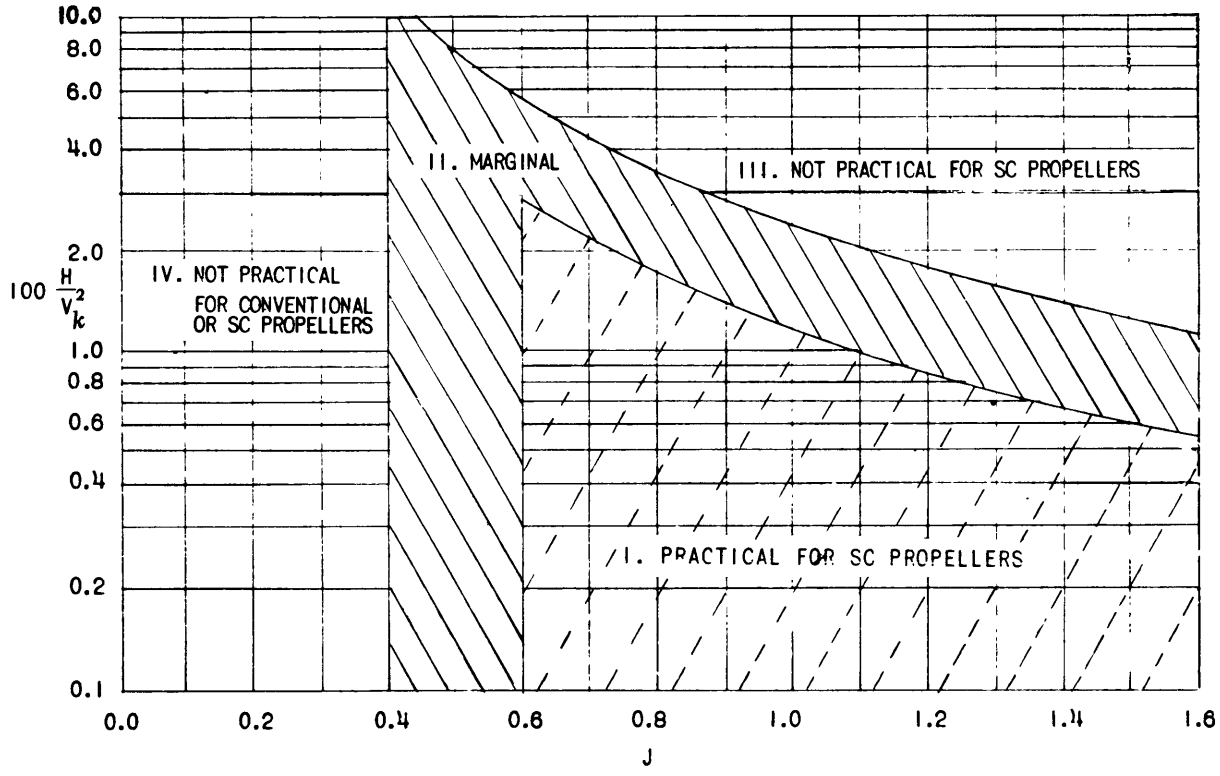

Figure 1 - Chart of Practical Application of Supercavitating Propellers

3. The chord l should be as large as possible, up to a certain limit, in order to decrease the nominal stresses.

4. For high efficiency, the design angle of attack should be small to give optimum lift-drag ratios.

5. For least stress, the design angle of attack should be large, giving a large cavity and so allowing the use of thick section shapes.

The above considerations, therefore, must all be examined to find an optimum propeller of a certain diameter and given number of blades. Similar investigations must also be made over a range of diameters and different numbers of blades.

DESIGN METHOD

The use of SC sections designed for best efficiency at no greater angle of attack than that necessary to prevent face cavitation leads to a thin cavity, and may result in leading edge vibration or blade failure. Figure 2 shows the cavitation pattern on a blade under severe vibration conditions and Figure 3 shows a propeller that failed due to overstressing. This problem of stress and vibration was partially overcome by increasing the section thickness on the cavity side from the nose to 50 percent of the length. This thicker section was determined by a series of tests on Propeller 3510. Figure 4 shows a comparison of this section with that calculated from theoretical considerations. In order to further decrease the nominal stress a design angle of attack somewhat larger than desirable from the standpoint of efficiency was used together with a very high strength material. The propellers have been manufactured from

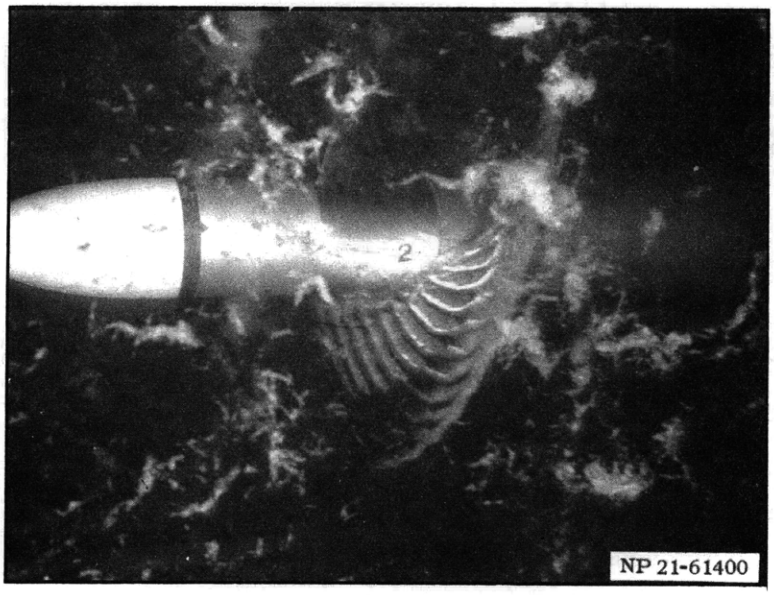

Figure 2 - Propeller 3460 Showing Effect of Blade Vibration on Cavitation

V_a = 50 fps, σ = 0.184, J = 0.935

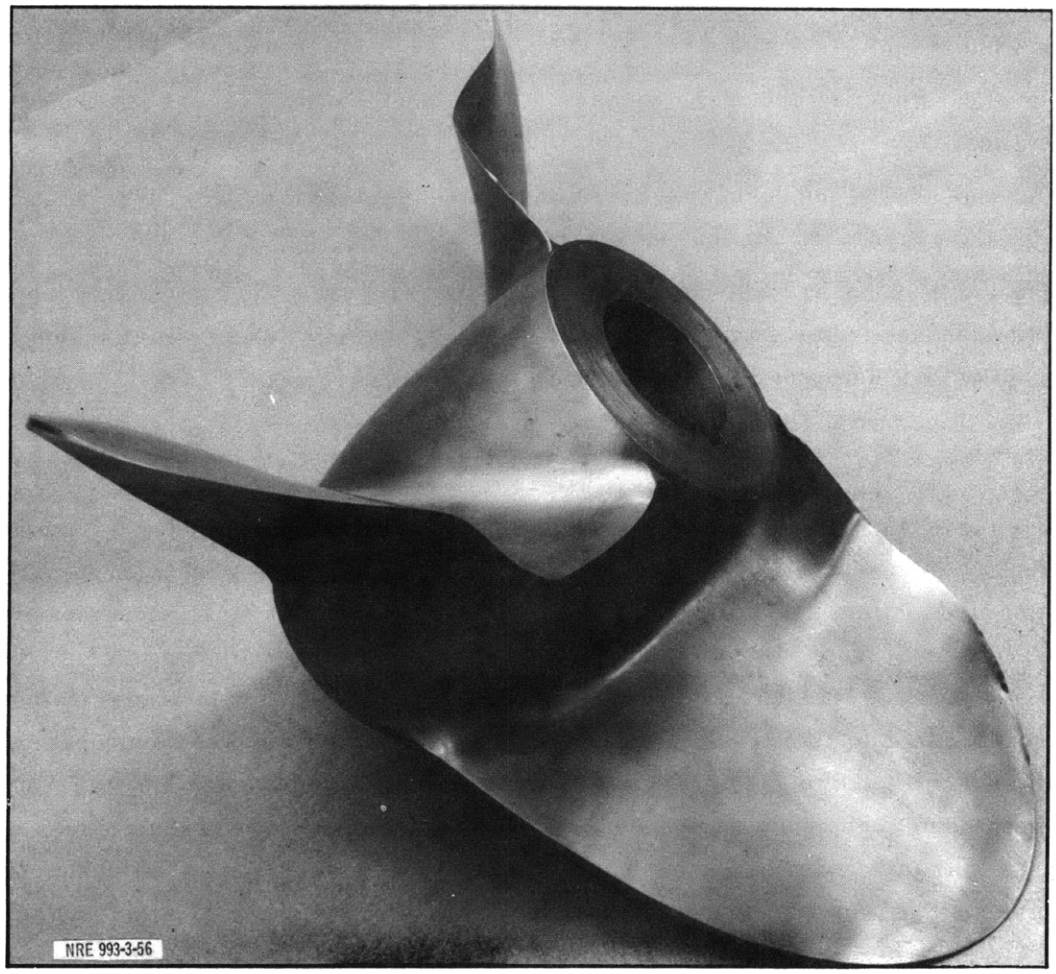

Figure 3 - Propeller 3509 after Failure from Overstressing

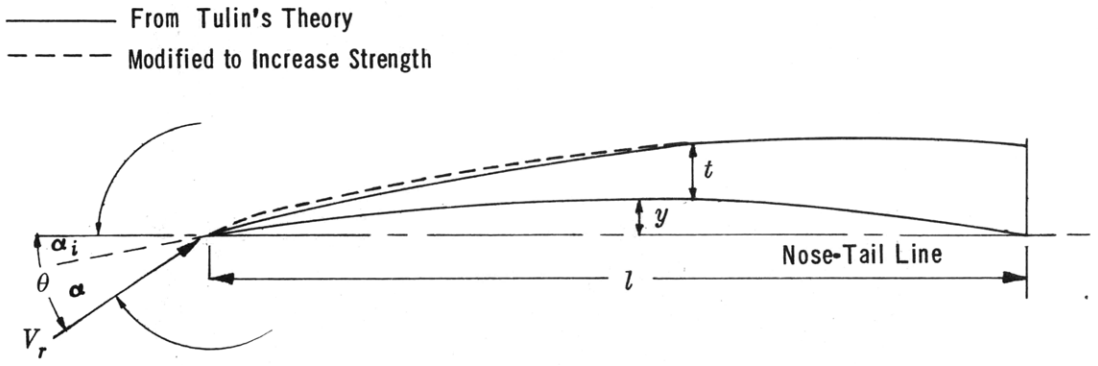

Figure 4 - Supercavitating Section Calculated from Equations [4] and [6] Compared to Section Calculated from Equations [4] and [7]
$C_L = 0.2$, $\alpha = 2$ degrees.

a stainless steel, type 420, which has a tensile strength of approximately 140,000 psi at a Rockwell "C" hardness of 30. A designed nominal stress of 30,000 psi has been found to give satisfactory results.

The ordinates of the pressure side of the section are given by the following formula:

$$\frac{y}{l} = x_l \sin\theta + \left[A_1\left(\frac{x_l}{2} + \frac{4}{3}\,x_l^{3/2} - 2x_l^{2}\right) - \frac{\alpha}{57.3}\,x_l\right]\cos\theta \qquad [2]$$

where

A_1 $= \frac{8}{5\pi}\,C_{L_0}$

C_{L_0} $= C_L - \frac{\pi}{114.6}\,\alpha$ is the lift coefficient from camber

C_L is the design lift coefficient,

θ $= \frac{\alpha + \alpha_i}{57.3}$ is the geometric angle of attack in radians,

α is the design angle of attack in degrees,

α_i is the ideal angle of attack in degrees,

y is the face ordinate measured perpendicular to the nose-tail line,

x_l is the fractional distance along the chord measured from the leading edge, and

l is the chord length.

The above equation can be simplified to

$$\frac{y}{l} = x_l \sin\theta + (B\,C_L - E\alpha)\cos\theta \qquad [3]$$

where B and E are coefficients from Table 1.

If θ is less than 0.1 radian, then $\sin\theta \doteqdot \theta$ and $\cos\theta \doteqdot 1$ and Equation [3] becomes

$$\frac{y}{l} = \theta\,x_l + B\,C_L - E\alpha \qquad [4]$$

and

$$\theta = 0.0849\,C_L + 0.01512\,\alpha \qquad \text{(radians)} \qquad [5]$$

The thickness of the cavity obtained theoretically is given by

$$\frac{t}{l} = F\,C_L + N\alpha \qquad [6]$$

TABLE 1

Coefficients for Obtaining Ordinates of SC Section

x_l	B	E	F	N	F'	N'
0	0	0	0	0	0	0
0.0075	0.00229	0.000194	−0.000663	0.000626	−0.001326	0.001254
0.0125	0.00397	0.000327	−0.001287	0.000935	−0.002574	0.001870
0.05	0.01778	0.001360	−0.008408	0.002852	−0.016816	0.005704
0.10	0.03675	0.002752	−0.01982	0.005052	−0.039520	0.010074
0.20	0.07094	0.005435	−0.04069	0.008943	−0.078940	0.017349
0.30	0.09631	0.007875	−0.05419	0.012339	−0.097600	0.022222
0.40	0.11067	0.010014	−0.05765	0.015299	−0.092870	0.024647
0.50	0.11281	0.011817	−0.04981	0.017842	−0.071780	0.025710
0.60	0.10171	0.013258	−0.02913	0.019948	−0.037750	0.025853
0.70	0.07685	0.014322	0.00502	0.021626	0.005940	0.025605
0.80	0.03769	0.014992	0.05276	0.022876	0.056880	0.024660
0.90	−0.01609	0.015264	0.1152	0.023687	0.112090	0.023047
0.95	−0.04859	0.015246	0.1516	0.023939	0.139620	0.022048
1.00	−0.08490	0.015123	0.1919	0.024066	0.166950	0.020937

PROP NO	DIA IN.	PITCH IN.	PITCH RATIO	NUMBER OF BLADES	EXP BLADE AREA	EXP AREA RATIO	MEAN WIDTH RATIO	PROJ AREA	PROJ AREA RATIO	BLADE THICKNESS FRACTION	RAKE ANGLE	ROTATION
3460	12.000	13.284	1.107	2	27.987	.247	.259	22.440	.198	.017	NONE	L.H.

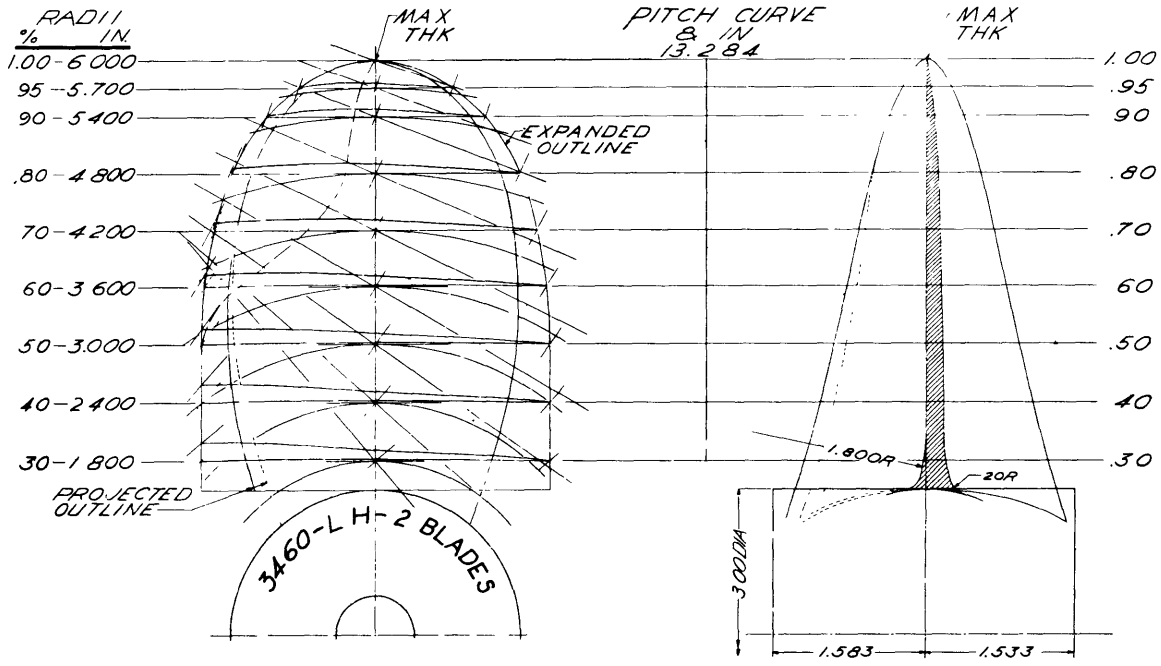

Figure 5 - Drawing of Propeller 3460

where t is the cavity thickness and F and N are constants obtained from Table 1. This equation has been modified to give a resulting section somewhat thicker near the leading edge. The following equation should, therefore, be used for determining the section thickness:

$$\frac{t}{l} = F' C_L + N' \alpha \qquad [7]$$

F' and N' are from Table 1.

The section resulting from Equations [4] and [7] has a finite trailing edge as shown in Figure 4.

In order to obtain good backing characteristics, the trailing edge should be thinned where possible. The sections toward the root must be thick for strength purposes, but at other sections the stress may decrease so that the trailing edge may be thinned. Figure 5 is a drawing of Propeller 3460 showing how the outer sections have been arbitrarily thinned towards the trailing edge.

The propeller design is carried out by following the method given in Reference 6. From the optimum circulation distribution, the hydrodynamic pitch angle can be calculated which in turn allows the quantity $C_L l/D$ to be determined for different radii. The lift coefficient C_L can then be determined by assuming a blade outline and the ordinates of the face and back can be calculated from Equations [4] and [7] for a desired angle of attack α.

The face ordinates as obtained from Equation [4] will give the design lift in rectilinear flow and they must, therefore, be changed in order to correct for the curvature of flow past the section. The correction coefficients given in Figure 7 of Reference 6 can be used for SC sections due to the coincidence of the camberline and face ordinates for these sections. This curvature correction does not include the friction correction, but it has been determined from experimental results that friction of the section has a negligible effect on the lift. It is, however, necessary in this case to incorporate a correction for a finite cavitation number.

The first addition in pitch embodies the design and ideal angles of attack. This is given by Equation [5] or in the notation used in Reference 6 as

$$\alpha_1 = K\theta = K(0.0849 C_L + 0.01512\alpha)\,57.3 \qquad [8]$$

The coefficient K is the correction arising from the fact that the propeller is operating at a finite cavitation number. It is obtained from Figure 6 where $\sigma_{0.7}$ is the section cavitation number at $0.7R$.

The additional angle of attack α_2 is calculated by assuming

$$\alpha_0 = 0 \qquad [9]$$

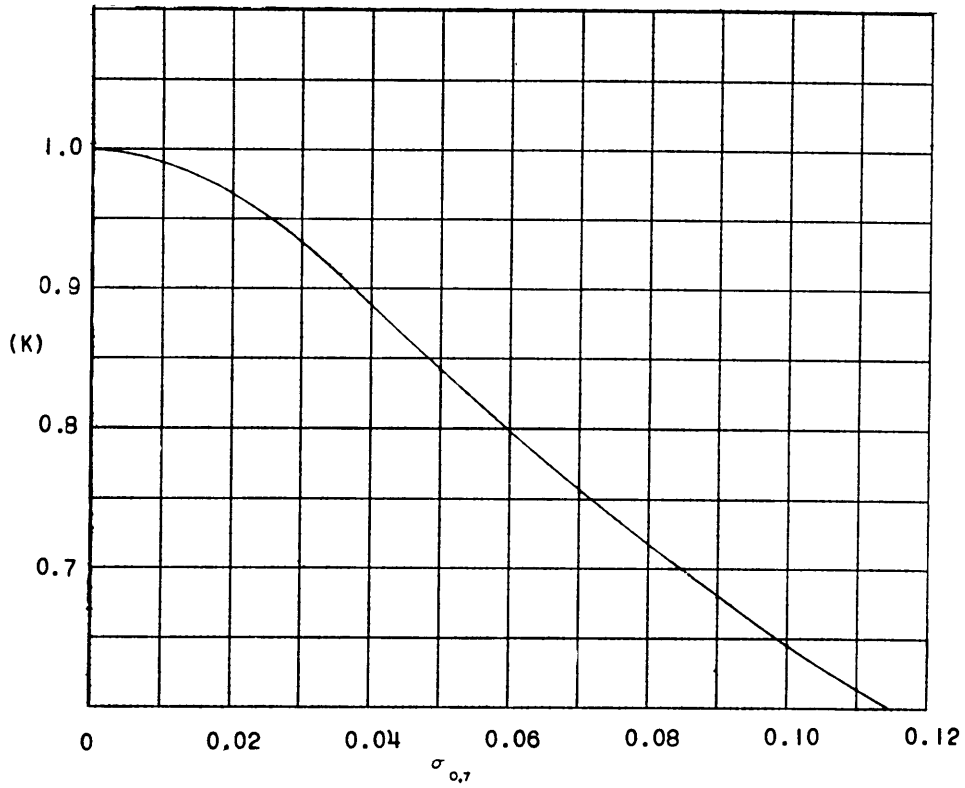

Figure 6 - Correction to θ for Finite Cavitation Number

This pitch correction is made at 0.7 radius and then the same percentage change applied to the other radii:

$$1 + \frac{\Delta P/D}{P/D} = \frac{\tan (\beta_i + \alpha_2)}{\tan \beta_i} \qquad [10]$$

The final pitch can now be computed:

$$\frac{P}{D} = \pi x \left(1 + \frac{\Delta P/D}{P/D}\right) \tan (\beta_i + \alpha_1) \qquad [11]$$

The propeller strength must be checked and the maximum allowable stress should be limited to not more than 30,000 psi for type 420 stainless steel. If the stresses are too high, the section characteristics must be adjusted. This can be accomplished by increasing the angle of attack, increasing the section length, changing the propeller diameter, or increasing the number of blades. It must be remembered, however, that for best efficiency the blades should be as few, and usually as narrow, as possible.

In order to obtain the torque per blade, it is necessary to estimate the drag-lift ratio ϵ

of each section by computing the potential and friction drags. The potential drag is given by the following formula:

$$(C_D)_p = \frac{(0.4C_L + 0.0164\alpha)^2}{1.5708} \qquad [12]$$

and the friction drag is approximated from Schoenherr[9] or by

$$(C_D)_f = \frac{0.455}{\left[\log_{10} \frac{V_r l}{\nu}\right]^{2.58}} \qquad [13]$$

where ν is the kinematic viscosity, and V_r is the inflow velocity to section $= \dfrac{x\pi nD - \frac{u_t}{2}}{\cos \beta_i}$

The total drag coefficient is then given by

$$C_D = (C_D)_p + (C_D)_f \qquad [14]$$

From experimental results it has been determined that this drag is at least 25 percent low. With this correction the drag-lift ratio of each section becomes

$$\epsilon = 1.25 \frac{C_D}{C_L} \qquad [15]$$

Once the design is completed the performance of the propeller can be determined. Three propellers which were designed by this method have been tested and all met the design conditions. Not enough experimental data, however, are available to ascertain that this method is completely satisfactory. It is anticipated that some improvement will be made when more two-dimensional data on the SC sections become available.

EXPERIMENTAL RESULTS

PROPELLER 3460

This was the first SC propeller designed using Tulin's low-drag SC section. It was designed for 65 knots, 680 lb thrust, and 7040 rpm for a diameter of 12 inches and has a constant pitch. In nondimensional terms, these conditions result in a speed coefficient J of 0.935, a thrust coefficient K_t of 0.0255, and a cavitation index σ of 0.184. This cavitation index is based upon the propeller speed of advance and the shaft centerline pressure. The physical characteristics of the propeller designed to these conditions are given in Figure 5.

Performance of this propeller was completely satisfactory in regard to efficiency and fulfillment of the design conditions. From Figure 7 it can be seen that rpm is only about one percent high at the design conditions. Also it should be noted that at cavitating conditions the K_t and K_q curves have very nearly a zero slope. This may lead to a low efficiency over part of the speed range when the propeller operates over a large range of J, such as on a hydrofoil boat.

There is a transition region shown on the curves between J of 1.1 and 1.0 where the cavitation shifts from the pressure face to the back of the blades. The lower efficiency e of the cavitating propeller in this region is due to the presence of face cavitation. After the bubble on the back of the blade becomes fully developed the curves become quite smooth. Typical tests of heavily cavitating conventional propellers often show quite a scatter in experimental points. This, however, was not true with the SC propeller as can be seen in Figures 8 to 12 which show little scatter of the experimental points. Figure 13 shows the open water test results and the results of the water tunnel atmospheric pressure test. Atmospheric pressure over the water in the tunnel test section along with a relatively low water speed resulted in a high cavitation index and only a little cavitation.

Figure 14 presents a cross plot of the foregoing curves showing the relationship of K_t, K_q, and e to the cavitation number at a constant J. This shows that while cavitation has a great effect upon thrust and torque, it has little effect upon efficiency. With a conventional propeller the efficiency would be expected to decrease at a low cavitation number. *The fact that there is a decrease of thrust with a decreasing cavitation number is not important as long as the efficiency remains constant and it is possible to meet the design conditions.*

This propeller exhibited extreme leading edge vibration, Figure 2, which led to singing at all conditions except design. To correct this vibratory condition, the section lengths were decreased 7 percent by cutting back the leading edges, which improved the vibration pattern considerably, as is shown in Figure 15. The nonuniformity of the cavity as shown in the figure is caused by the cavity not forming at a uniform distance from the leading edge. Figure 16 shows that at the design conditions the efficiency dropped by about 9 percent. Consequently, it was concluded that this method of preventing blade vibration was unsatisfactory.

To complete the study on this propeller, tests were run to determine the effect of a finite trailing edge on the backing performance of the propeller. Figure 17 shows that the efficiency of this propeller while back driving is relatively good and is as high as that of a noncavitating backing conventional propeller. It is believed that this high efficiency is due to cavitation forming on the back of the blade at the finite trailing edge which is in this condition the leading edge. This would considerably improve the flow in this region and thus reduce the drag.

Text continued on page 20.

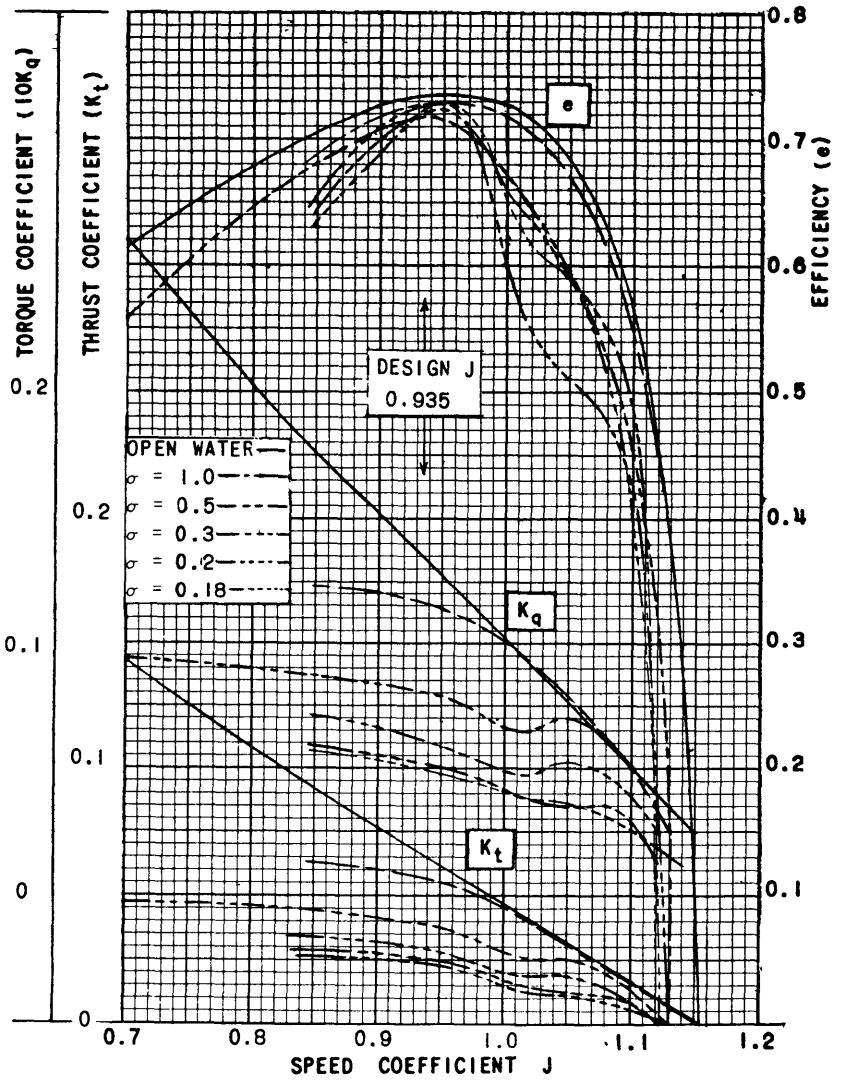

Figure 7 - Composite Plot of Tests on Propeller 3460

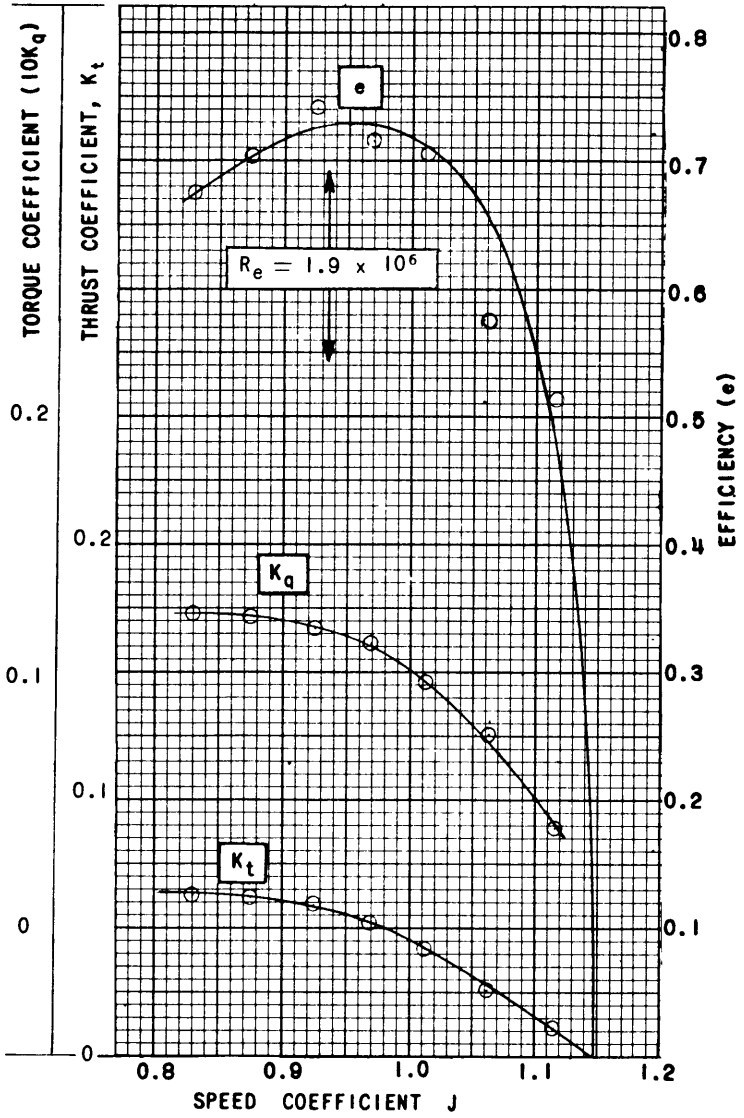

Figure 8 - Characteristic Curves of Propeller 3460 at $\sigma = 1.0$

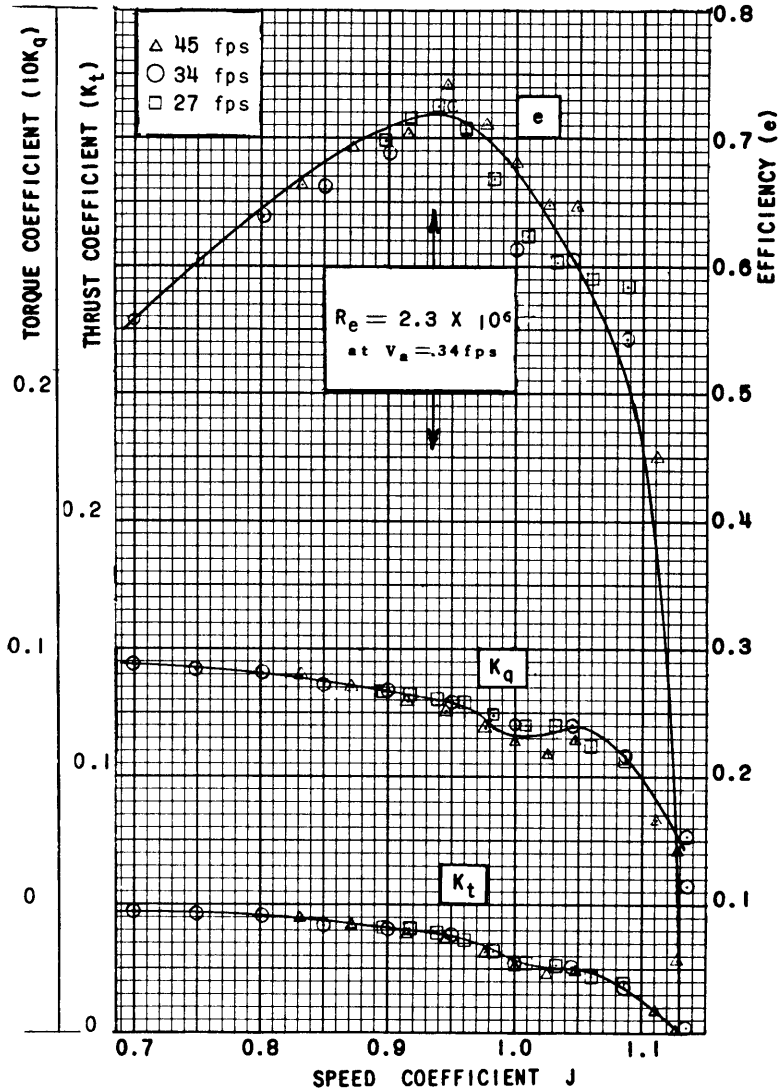

Figure 9 - Characteristic Curves of Propeller 3460 at $\sigma = 0.5$

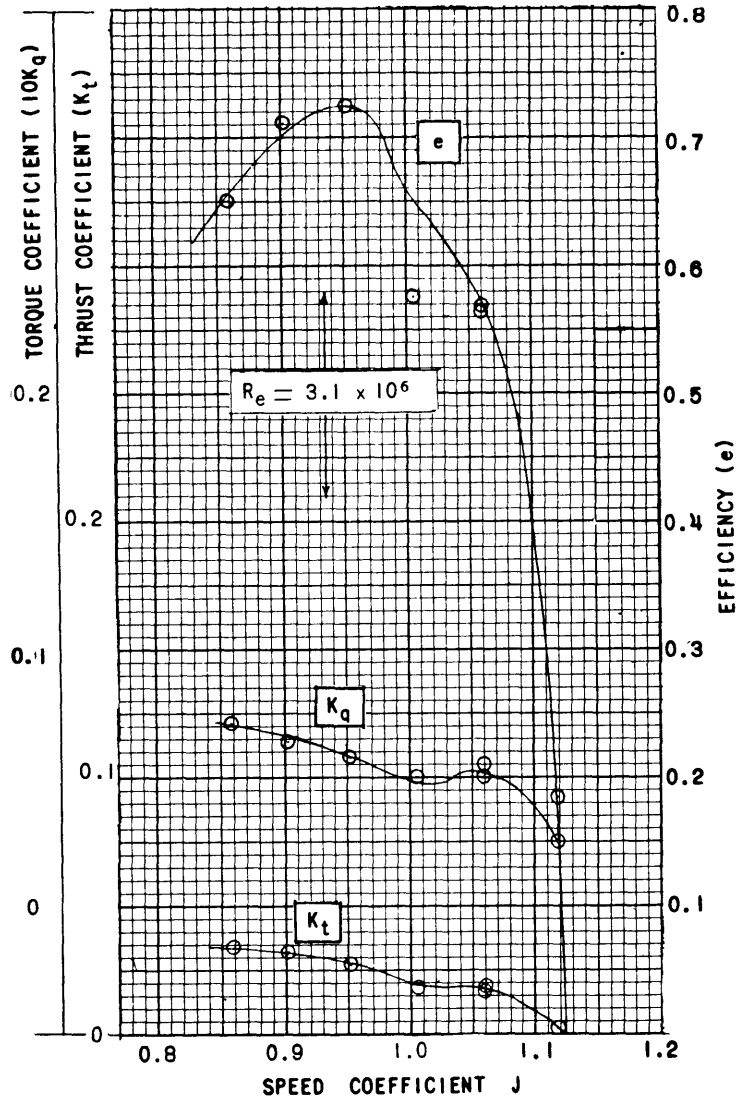

Figure 10 - Characteristic Curves of Propeller 3460 at $\sigma = 0.3$

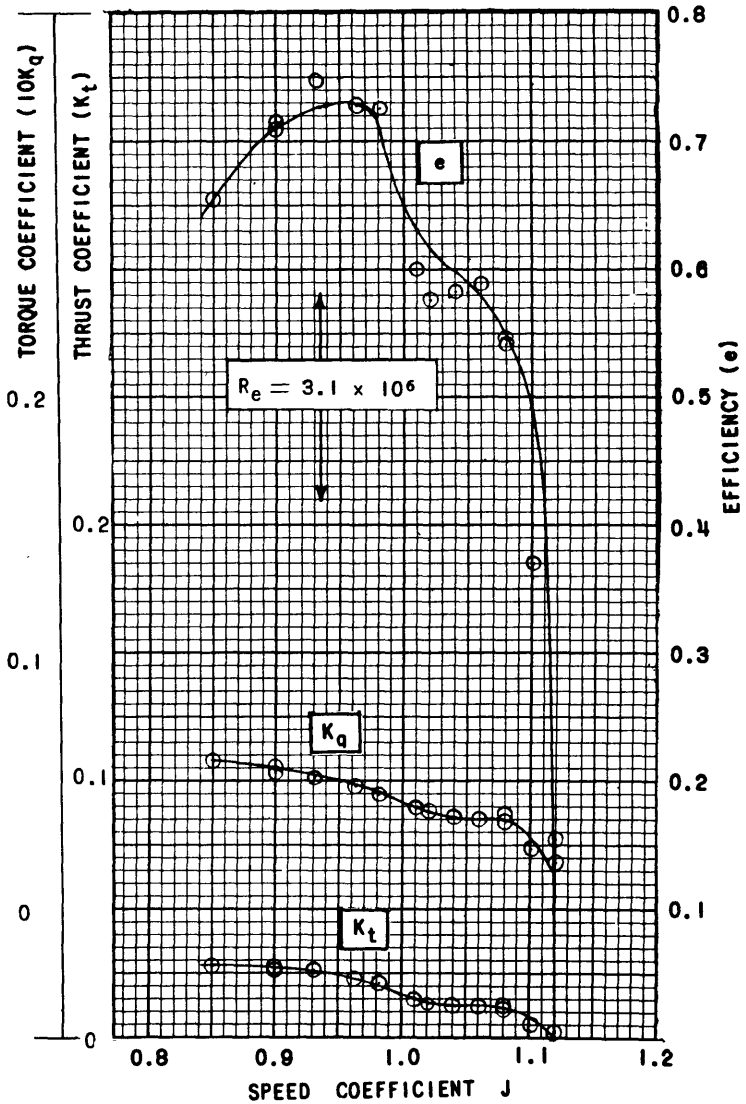

Figure 11 - Characteristic Curves of Propeller 3460 at $\sigma = 0.2$

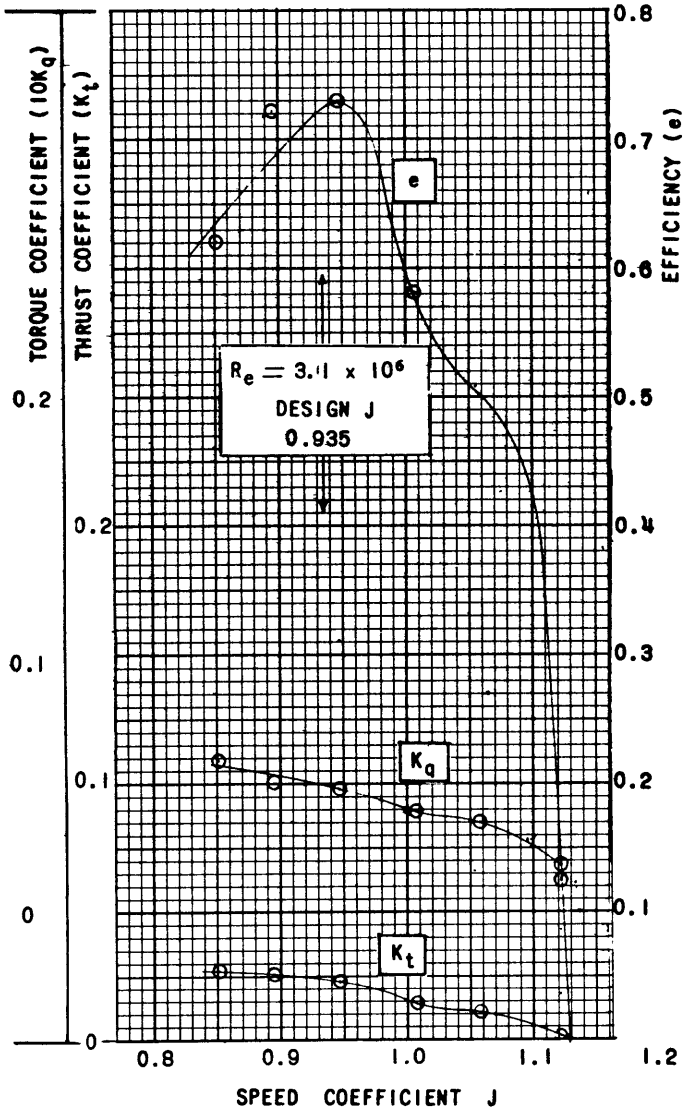

Figure 12 - Characteristic Curves of Propeller 3460 at $\sigma = 0.18$

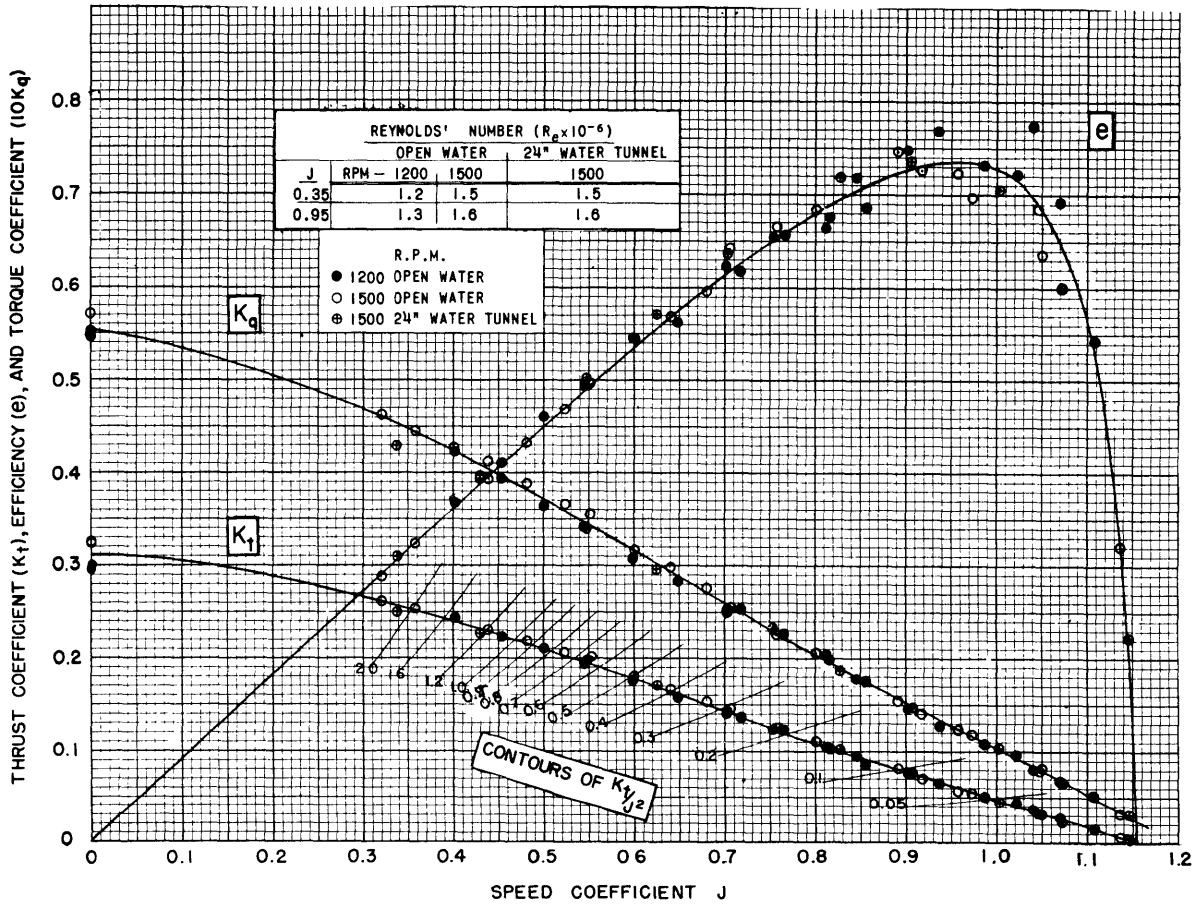

Figure 13 - Open-Water and Atmospheric-Tunnel Characteristic Curves of Propeller 3460

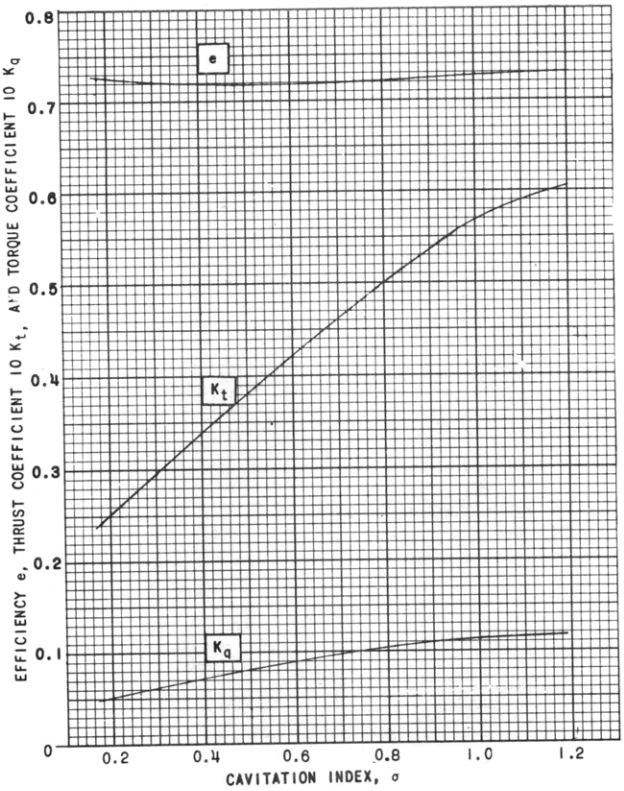

Figure 14 - Plot of K_t, K_q, and e versus σ for Propeller 3460 at Design J ($J = 0.935$)

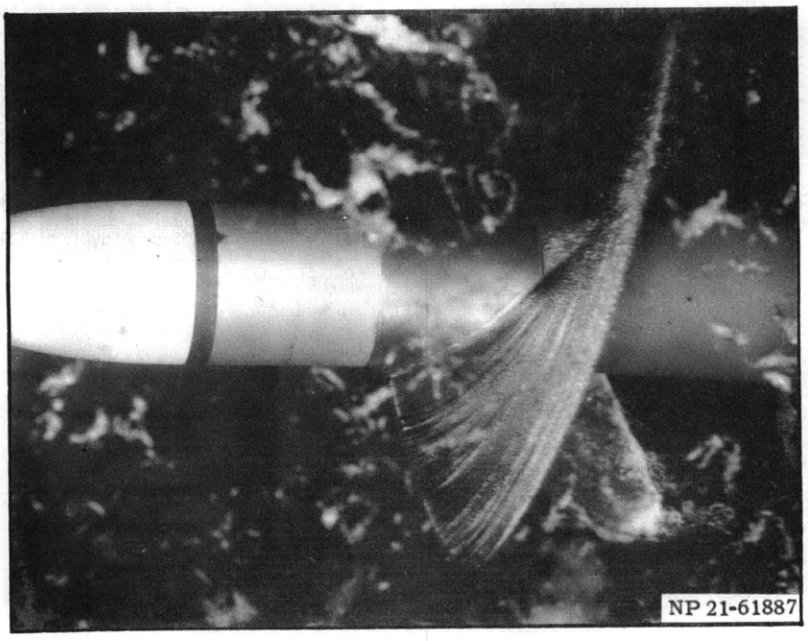

Figure 15 - Propeller 3460 with Leading Edge Cut Back 7 Percent

$V_a = 45$ fps, $\sigma = 0.184$, $J = 0.935$.

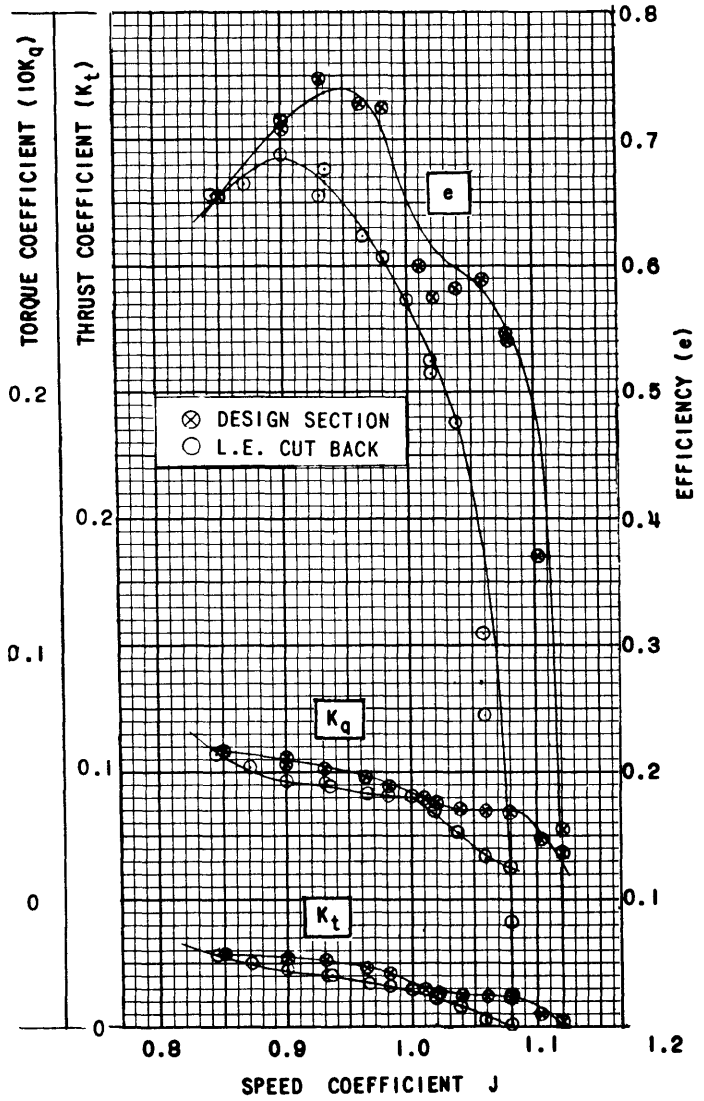

Figure 16 - Comparison of Characteristic Curves of Propeller 3460 with and without Leading Edge Cut Back at $\sigma = 0.2$

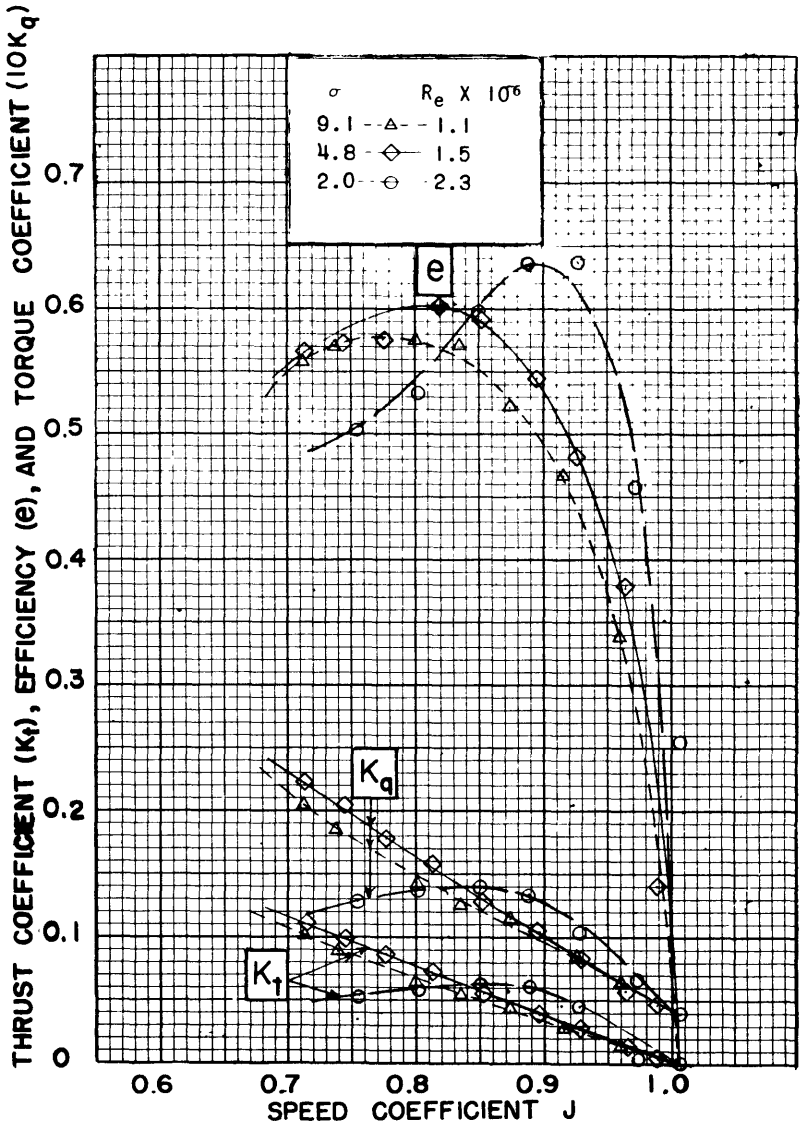

Figure 17 - Backing Characteristic Curves of Propeller 3460

PROPELLER 3509

A propeller was designed for the Canadian hydrofoil boat R-100 to check the scale effect for fully cavitating flows and the operation characteristics of a full-scale SC propeller. This vessel, which is a research craft operated by the Naval Research Establishment, Dartmouth, Nova Scotia, has a displacement of 8.5 tons and length of 45 feet, and was utilized because of its available instrumentation for measuring thrust, torque, and rpm. The propeller was designed for 50 knots, 3500 lb thrust, and 3000 rpm with a diameter 18 inches. Using nondimensional coefficients these conditions result in a thrust coefficient of 0.140, speed coefficient of 1.125, and cavitation number of 0.307. The physical characteristics of the propeller are given in Figure 18.

This propeller failed from overstressing, Figure 3, when tested on the craft, and the performance characteristics could not be obtained. Failure occurred at about the 0.7 radius and resulted from a high wake region generated by a lifting foil ahead of the propeller, Figure 19.

These overstressed conditions were anticipated when the model of this propeller was tested and a second propeller was built, No. 3604, which was immediately available for testing on the craft.

PROPELLER 3510

This propeller was a 14-inch model of 3509. Tests of the first SC propeller indicated that the sections were prone to leading edge vibration. The previous attempt to alleviate this problem was unsatisfactory, and as a result Propeller 3510 was manufactured in four stages to determine the performance of thicker SC sections. These new sections had the same face ordinates but with varying thickness distributions. Differences in the sections are defined by a percentage increase in thickness over the design value as obtained from 3509 and measured at 5 percent of the section length and faired towards leading and trailing edges. Propeller 3510A was 100 percent thicker at this point; 3510B was 50 percent thicker; 3510C was 25 percent thicker; and 3510 has the design thickness. Figure 4 shows a comparison of the 0.7 radius section of Propeller 3510A with that of 3510.

Propeller 3510A was satisfactory from the standpoint of vibration whereas the propellers with thinner sections exhibited some objectionable leading edge vibration. The performance characteristics of all these propellers, however, were satisfactory and met the design conditions, although it had been expected that the thicker sections would result in a lower efficiency. The results are shown in Figures 20, 21, and 22.

On the basis of these tests it was decided that the cavity thickness distribution as obtained from Equation [6] could be modified without greatly impairing the lift-drag ratio and cavitation pattern of the section. The thickness distribution as given by Equation [7] has, therefore, been developed.

PROP NO	DIA IN.	PITCH IN.	PITCH RATIO	NUMBER OF BLADES	EXP BLADE AREA	EXP. AREA RATIO	MEAN WIDTH RATIO	PROJ AREA	PROJ AREA RATIO	BLADE THICKNESS FRACTION	RAKE ANGLE	ROTATION
3509	18.000	27.601	1.533	3	113.070	.444	.310	84.393	.332	VAR	NONE	RH

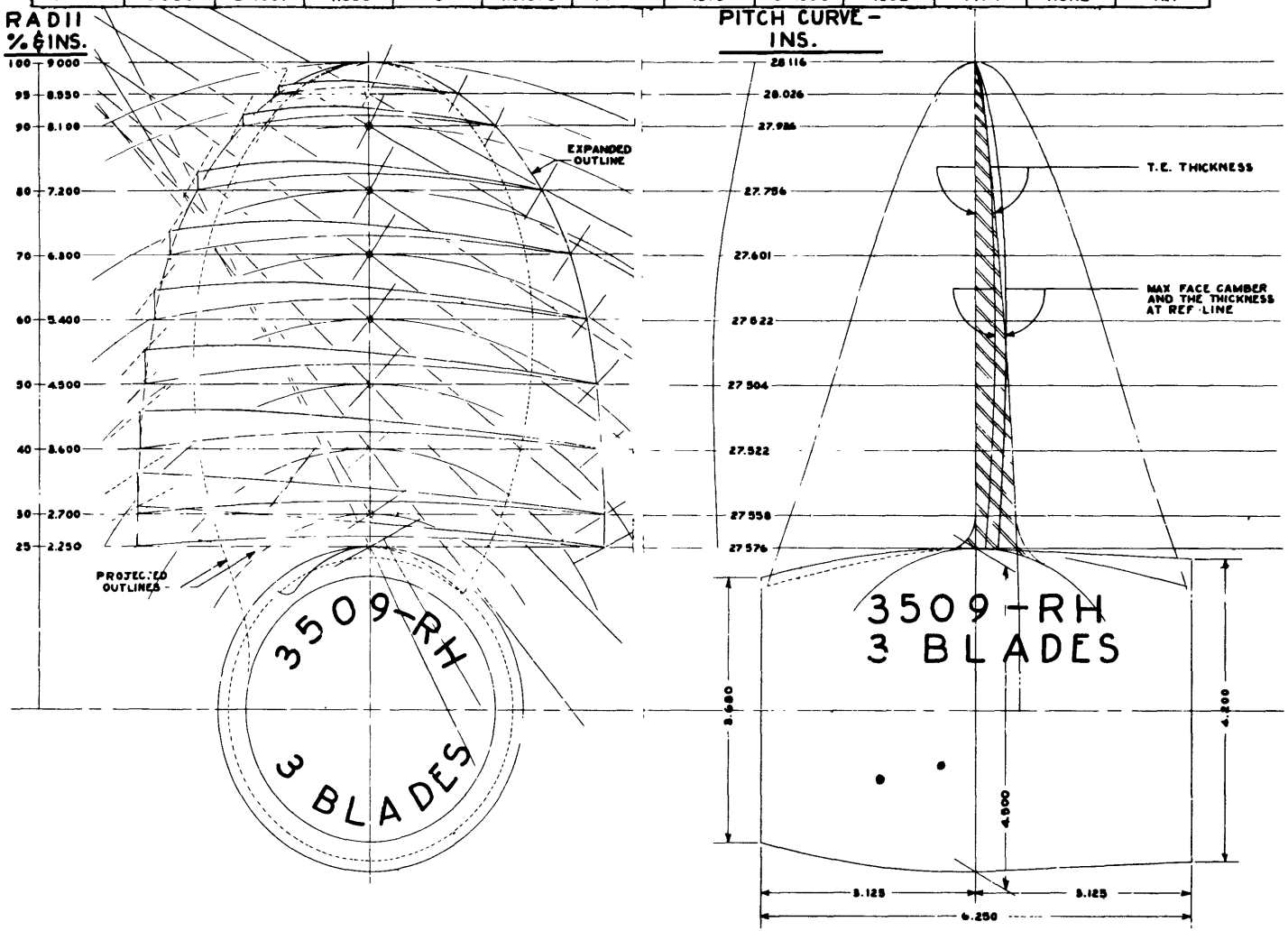

Figure 18 - Drawing of Propeller 3509

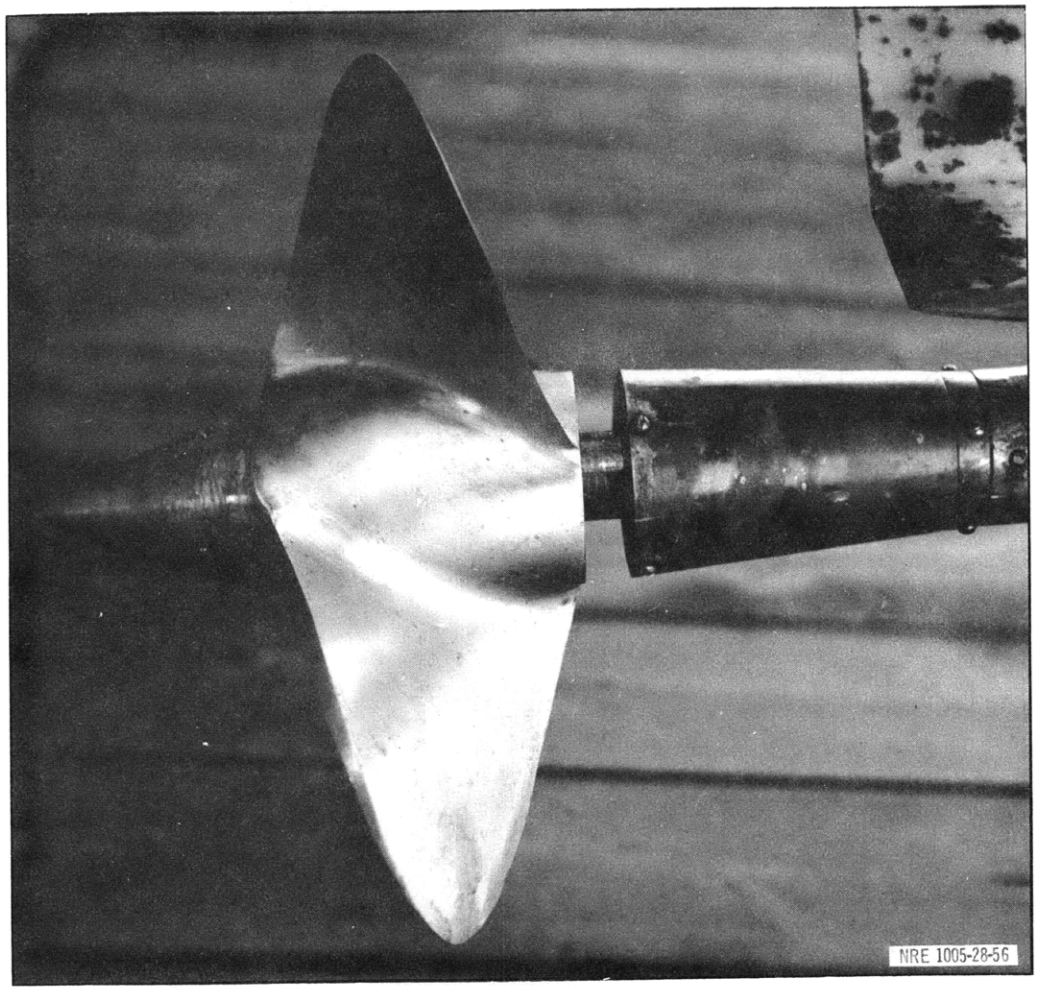

Figure 19 - Propeller 3604 Showing Position of Foil Forward of the Propeller

Figure 23 is a composite plot of Figures 20, 21, and 22 for various cavitation numbers and Figure 24 shows the open-water characteristics. The curves in Figure 23 show the same general behavior as those of Propeller 3460. From this figure it can be seen that at the design conditions the rpm is within 1 percent of the desired value. It was noticed that due to the high cavitation index for which this propeller was designed to operate, the cavity did not completely enclose the blade. As a result of these tests, it is now recommended that the section cavitation number at 0.7 radius be limited to a maximum of 0.045 for the cavity to collapse beyond the trailing edge.

As with Propeller 3460, a cross-plot, Figure 25, was made to determine the variation of K_t, K_q, and efficiency with σ at design J. The same remarks apply to this curve as to the one for Propeller 3460. Backing tests, Figure 26, were also run on the propeller and showed satisfactory performance.

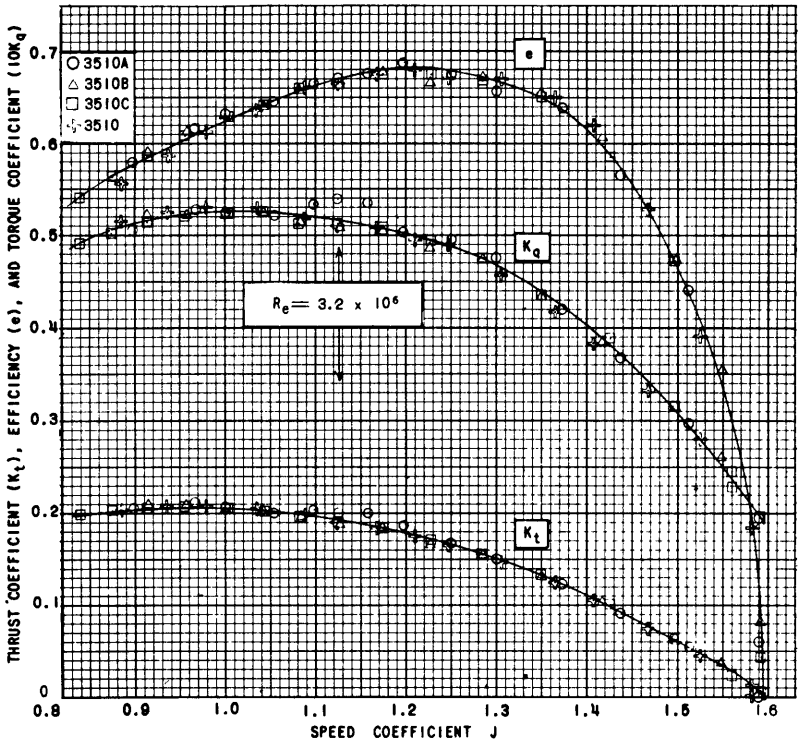

Figure 20 - Characteristic Curves of Propeller 3510 at $\sigma = 1.0$

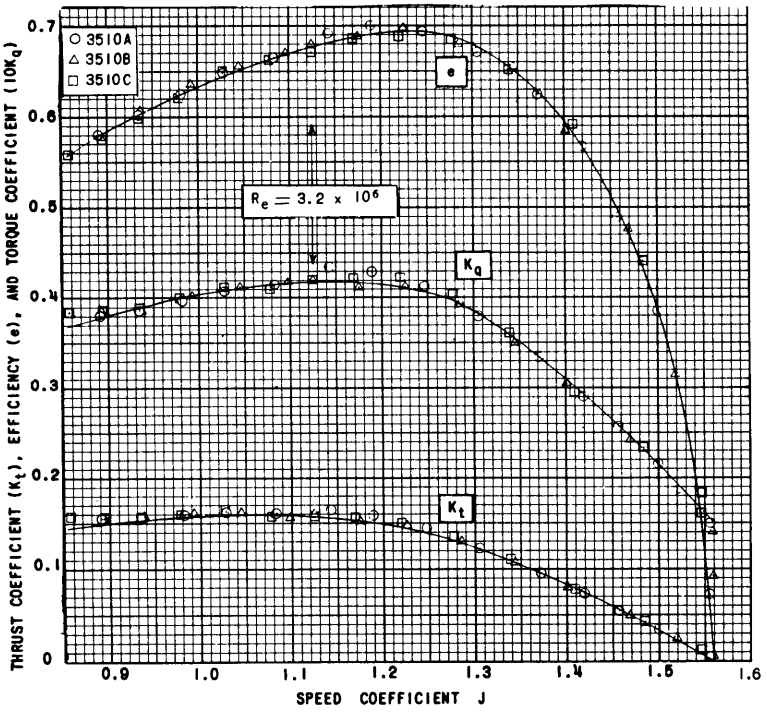

Figure 21 - Characteristic Curves of Propeller 3510 at $\sigma = 0.5$

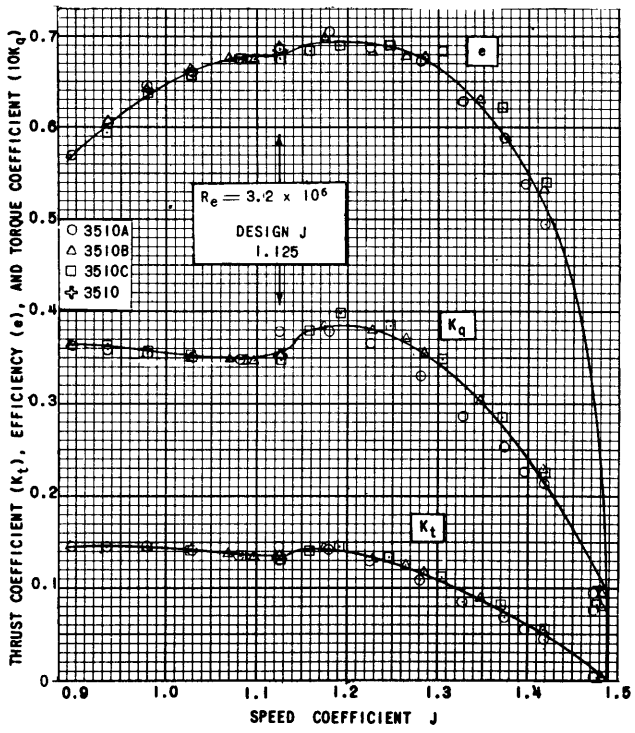

Figure 22 - Characteristic Curves of Propeller 3510 at $\sigma = 0.3$

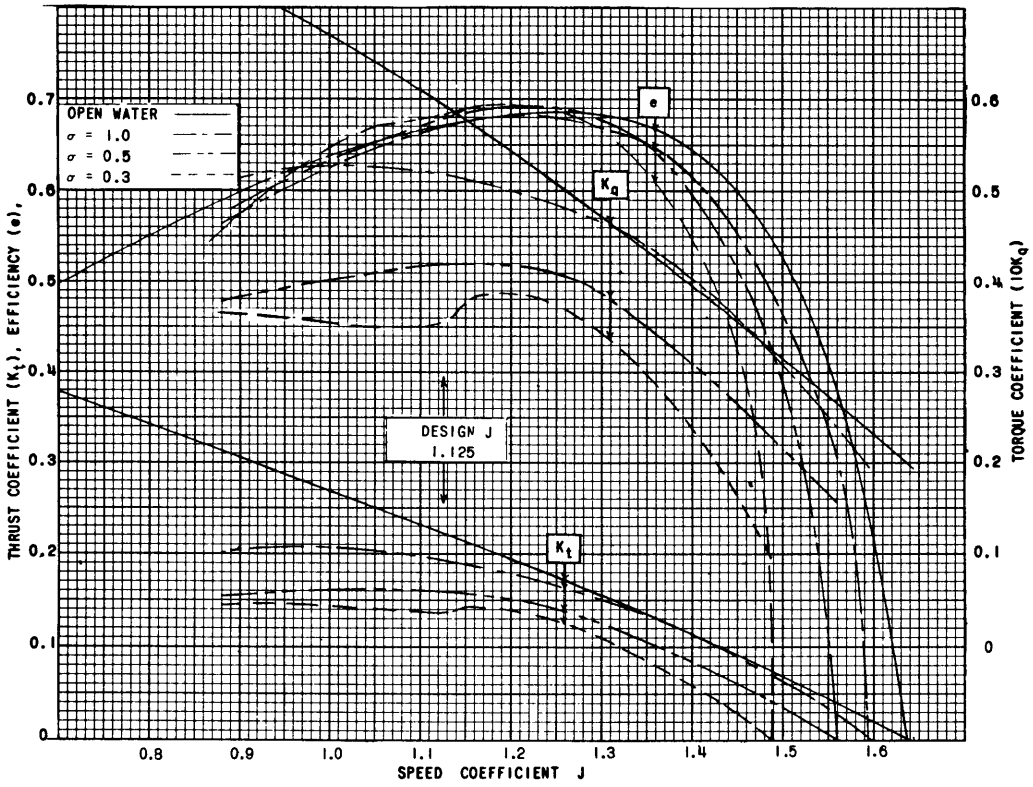

Figure 23 - Composite Plot of Tests on Propeller 3510

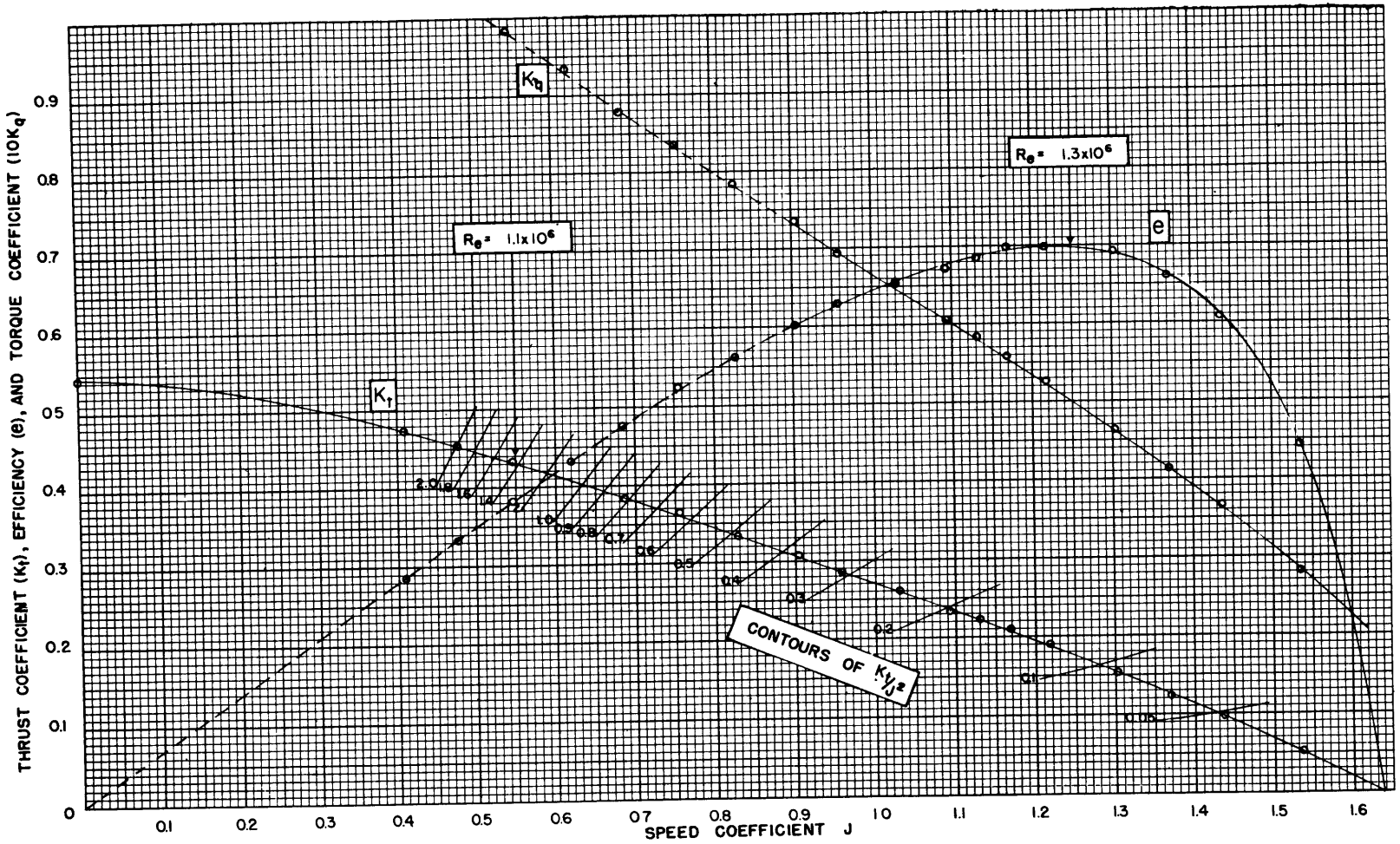

Figure 24 - Open-Water Characteristic Curves of Propeller 3510

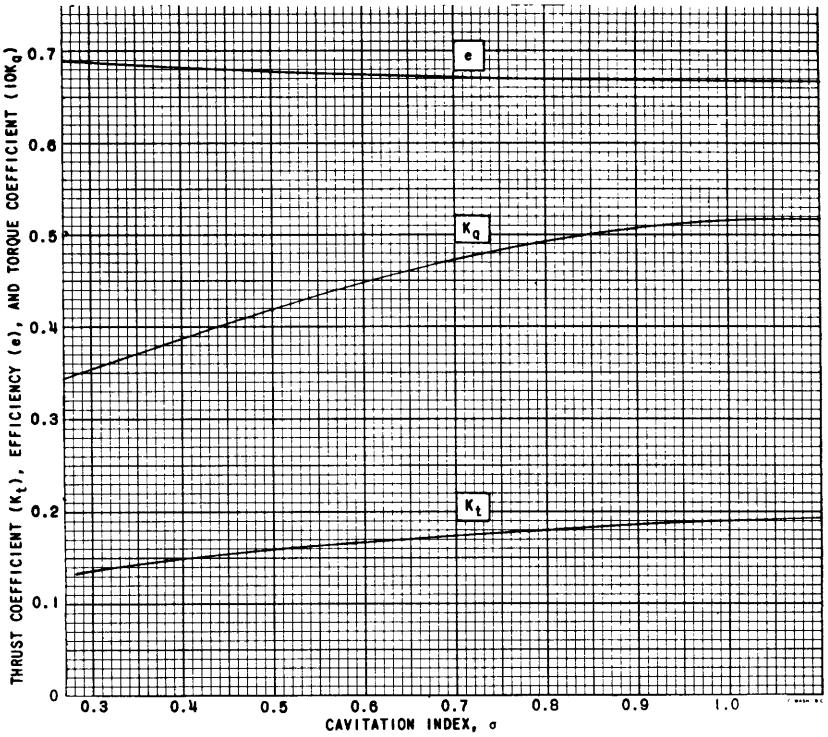

Figure 25 - Plot of K_t, K_q, and e versus σ for Propeller 3510 at Design J (J = 1.125)

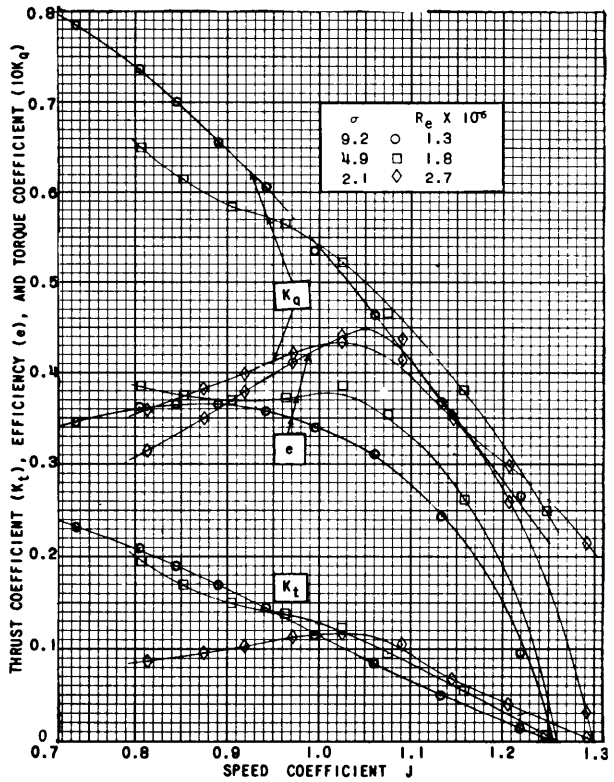

Figure 26 - Backing Characteristic Curves of Propeller 3510

PROPELLER 3604

This propeller was manufactured to replace 3509 and designed with the sections developed from 3510A. It was tested on the Canadian hydrofoil boat R-100 in Bedford Basin, Halifax, Nova Scotia. Bedford Basin is a salt water bay approximately 3 miles by 5 miles with an average depth of about 150 feet. These tests were conducted on the boat immediately after new hydrofoils had been installed and before they had been properly adjusted. Consequently, the hydrofoils ventilated at the higher speeds, resulting in a much higher drag than had been predicted. For this reason a thrust of 3500 lb was necessary at 40 knots instead of at the design speed of 50 knots. It is anticipated that when the foils are operating properly new tests will be conducted which will give results closer to the predicted value. Although this propeller was operating considerably off the design conditions, it performed quite satisfactorily. Figures 27a and 27b give the performance of Propeller 3604 when operating on the Canadian hydrofoil boat. Thrust and torque measurements were obtained at the engine and approximate corrections were necessary to determine the propeller conditions. It is estimated that the thrust and torque values are accurate to $\pm$ 5 percent while the speed and rpm are accurate to $\pm$ 2 percent. From Figures 27a, and 27b, at 40 knots the values of K_t, K_q, e, and J are 0.147, 0.0368, 0.572, and 0.90, respectively. The resulting σ at this speed is 0.49. From the characteristic curves of Model 3510, Figure 23, at this σ and J the values of K_t, K_q, and e are 0.155, 0.0378, and 0.584, respectively. The percentage differences between these values are considered to be well within experimental accuracy. It should also be noted that the full-scale propeller operated with a shaft angle of about 10 degrees to the flow.

Comparison, therefore, of the results of the Canadian test to those obtained in the 24-inch water tunnel indicate that the laws of similitude hold for fully cavitating flows.

The curves of Propeller 3604, Figures 27a and 27b, are typical of a hydrofoil craft except for the extreme increase in thrust and torque above 40 knots. This increase is due to a high drag caused by ventilation of the hydrofoils. Between 20 and 40 knots there is a large change in the propulsive coefficient, thp/shp, with speed. This corresponds to the small change in rpm which results in a large change in speed coefficient. With displacement craft the speed coefficient remains almost constant with speed and the problem of the propeller operating very inefficiently over a certain speed range does not occur.

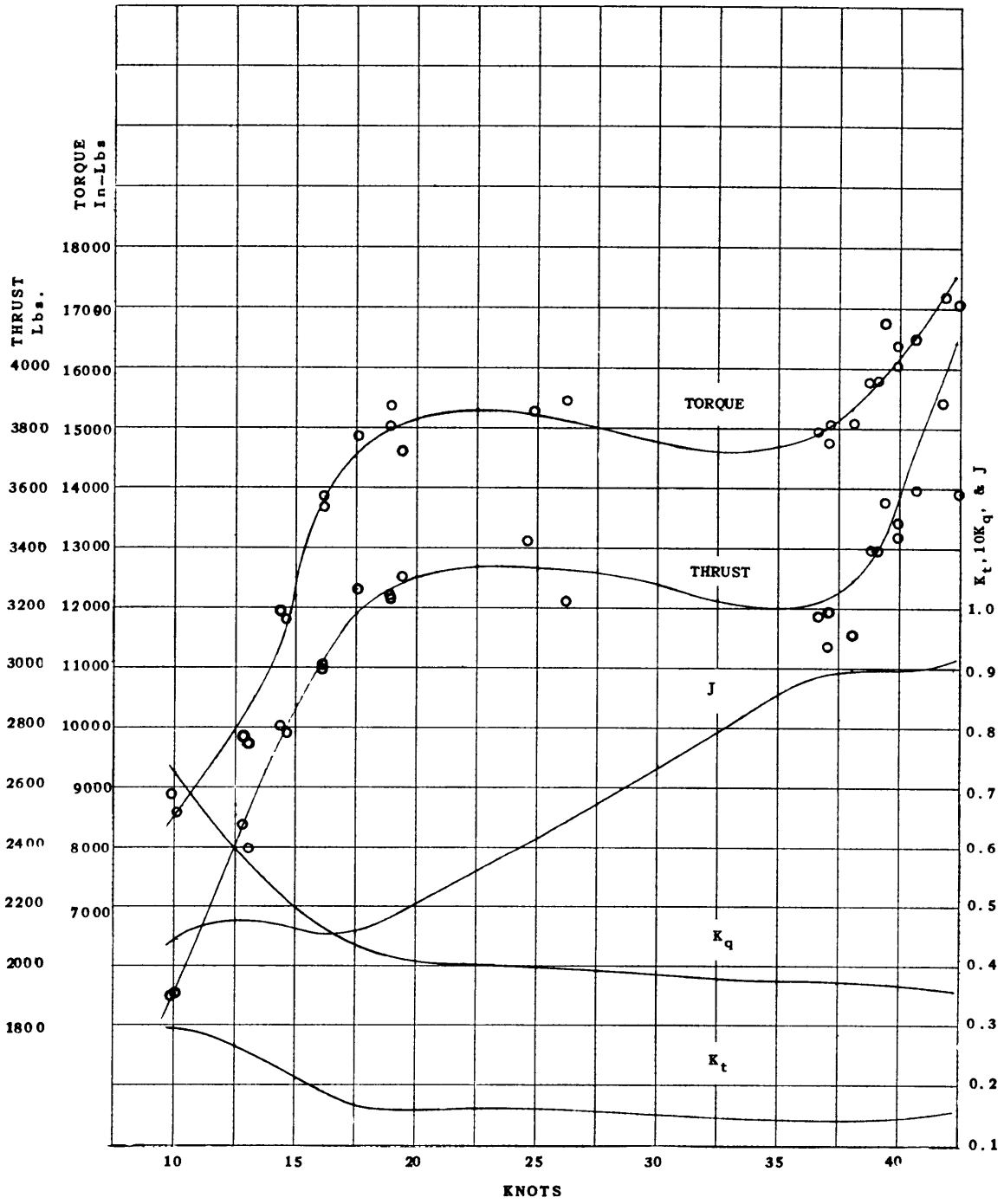
TORQUE In-Lbs
THRUST Lbs.
TORQUE
THRUST
J
K_q
K_t
K_t, $10K_q$, & J
KNOTS
18000
17000
16000
15000
14000
13000
12000
11000
10000
9000
8000
7000
4000
3800
3600
3400
3200
3000
2800
2600
2400
2200
2000
1800
1.0
0.9
0.8
0.7
0.6
0.5
0.4
0.3
0.2
0.1
10
15
20
25
30
35
40

Figure 27a -

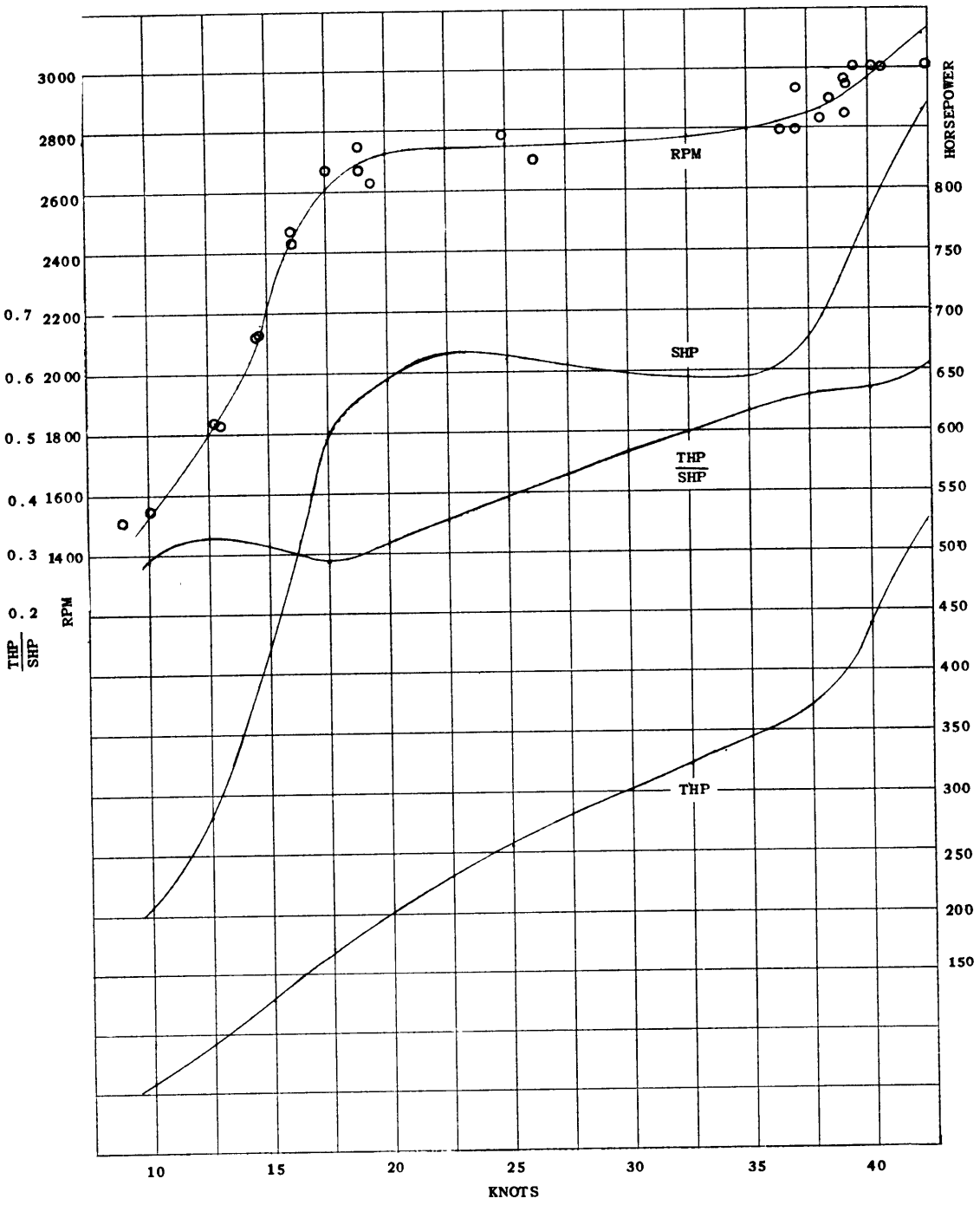

Figure 27b -

Figure 27 - Performance Characteristics of Propeller 3604 on Canadian Hydrofoil Boat R-100

CONCLUSIONS

The work completed to date has shown that SC propellers are feasible and their performance may show considerable improvement over cavitating conventional propellers for certain operating conditions. It appears that SC propellers should be restricted to the high speed ranges (above 50 knots) in order to derive the full benefit of their hydrodynamic performance. At lower speeds, SC propellers may be feasible for certain applications where conventional or contrarotating propellers are not practical because of cavitation.

The results obtained on model and full scale have indicated that this type of propeller exhibits great hydrodynamic advantages and that the SC sections characteristics can be used with good results. It has also been shown that it is possible to use available theoretical methods for the design and the determination of the operating characteristics. Furthermore, it has been verified that, for the propellers which have been tested, no measurable scale effect is present for fully cavitating flows and that the similitude laws between model and full scale are satisfactory.

The original objectives therefore have been achieved. However, considerable effort is needed to solve many of the problems that exist for the application of such propellers. The vibration problems, which were present in the application of the first designs and which it is hoped have been alleviated by the incorporation of thicker sections, have indicated the need for further effort to be expended along these lines. The magnitude of such effects as wake distribution and proximity of hull surface are yet unknown, particularly regarding the blade vibration characteristics.

The problem of high nominal stresses has indicated the need for a lifting surface strength theory which would take account of the chordwise distribution of blade loading.

The design procedure has given satisfactory results for the few designs which have been tested. Some improvements in this procedure, however, can be anticipated as more designs are accomplished and test results become available. It is also planned to investigate the effect of certain design parameters and determine optimum combinations of design features for best operating characteristics. Two-dimensional performance characteristics should be obtained on the modified Tulin low-drag section and compared with the original section. Knowledge regarding the extent of erosion on the blade and the noise characteristics when the cavity collapses beyond the trailing edge of the blade is also necessary in order to extend the possible range of application for such propellers.

ACKNOWLEDGEMENT

The test of the SC propeller on the Canadian Hydrofoil boat was conducted by the staff of the Naval Research Establishment, Dartmouth, Nova Scotia. Particularly the work of Mr. L. J. Payzant, Mr. M.C. Eames, Mr. E.A. Jones, and Mr. G.K. Naas in conducting this part of the program is gratefully appreciated.

REFERENCES

1. Tulin, M. and Burkart, M., "Linearized Theory for Flows about Lifting Foils at Zero Cavitation Number," David Taylor Model Basin Report C-638 (Feb 1955) CONFIDENTIAL.

2. Tulin, M., "Supercavitating Flow Past Foils and Struts," Paper No. 16, Symposium on Cavitation in Hydrodynamics, National Physical Laboratory, Teddington, England (1955).

3. Wu, T. Y., "A Free-Streamline Theory for Two Dimensional Fully Cavitated Hydrofoils," California Institute of Technology Report 21-17 (Jul 1955).

4. Hug, M., "Theoretical and Experimental Investigation of Forces on Cavitating Hydrofoils," Ph.D. Thesis, University of Iowa (Feb 1956).

5. Waid, R.L. and Lindberg, Z.M., "Water Tunnel and Theoretical Investigations of a Supercavitating Hydrofoil," California Institute of Technology, Hydrodynamics Report No. 47-8 (1956).

6. Eckhardt, M. and Morgan, W.B., "A Propeller Design Method," Transactions of the Society of Naval Architects and Marine Engineers (1955).

7. Ripken, J.F., "An Interim Report on Pressure Distribution Studies for a Supercavitating Hydrofoil," Memorandum M-46, St. Anthony Falls Hydraulic Laboratory (Dec 1955) CONFIDENTIAL.

8. Ripken, J.F., "An Interim Report on Pressure Distribution Studies for a Supercavitating Hydrofoil," Memorandum M-50, St. Anthony Falls Hydraulic Laboratory (Apr 1956) CONFIDENTIAL.

9. Gertler, M., "The Prediction of the Effective Horsepower of Ships by Methods in Use at the David Taylor Model Basin," David Taylor Model Basin Report 576 (Dec 1947).

INITIAL DISTRIBUTION

Serials

1-10 CHBUSHIPS, Library (Code 312)
- 1- 5 Tech Library
- 6 Prelim Des (Code 420)
- 7 Mach Des (Code 430)
- 8 Hull Des (Code 440)
- 9 Pro & Shafting (Code 554)
- 10 Sec Div (Code 205)
  For, ADM, US Maritime Adm.
  Attn: Tech Division

11-12 CHBUORD
- 11 Library (Code Ad3)
- 12 Res & Components (Code Re6a)

13-15 CHBUAER
- 13 Library (Code TD-42)
- 14 Aero & Hydro (Code AD-3)
- 15 Applied Math (Code RS-7)

16 CHNOP

17-20 CHONR
- 17-19 Mech Br (Code 438)
- 20 Undersea Warfare (Code 466)

21 CDR, USNOTS, Pasadena, Calif.

22 CDR, USNOL

23 DIR, USNRL

24 DIR, USNEES, Annapolis, Md.

25 CO, USNADC, Johnsville, Pa.

26 SUPT, USN Postgrad School, Monterey, Calif.

27 Asst. Secy for Defense (Res & Dev)

28 Sec of the Air Force (Res & Dev)

29 CG, Wright-Patterson AFB, Ohio
Attn: Office of Air Research

30 DIR, Langley Aero Lab, Langley, Va.

31 DIR, Aero Res, NACA

32 Gibbs & Cox, Inc, via SUPSHIPINSORD, New York, N.Y.

33 Head, Dept of NAME, MIT, via INSMAT, Boston, Mass.

34 Hydro Lab, CIT, via CO, ONR, Pasadena, Calif.

35 DIR, Iowa Inst of Hydraulic Res, State Univ of Iowa, Iowa City, Iowa, via CO, ONR, Chicago, Ill.

36 DIR, St. Anthony Falls Hydraulic Lab, Univ of Minn, via CO, ONR, Chicago, Ill.

37 Polytech Inst, Dept Aero & Appl Mech, via CO, ONR, New York

38 Pennsylvania State Univ, Ord Res Lab, via Dev Contr Admin, Univ Park, Pa.

39 Propulsion Res Corp, 1860 Franklin St., Santa Monica, Calif, via San Bernardino Air Materiel Area, Norton AFB, Calif.

40 Aerojet Gen Corp, via BAR, Azusa, Calif.

41 DIR, ETT, SIT, via ONR, New York

42-50 BJSM (NS)

51-53 CJS